RNA干渉法による治療を実現するための研究

野地　澄晴　徳島大学大学院ソシオテクノサイエンス研究部
足立　太郎　徳島大学大学院先端技術科学教育部
川上　恵実　徳島大学大学院歯学研究科
田中　栄二　徳島大学大学院ヘルスバイオサイエンス研究部

要旨

RNA干渉（RNA interference（RNAi））は，細胞内で二本鎖RNAと相補的な塩基配列を持つmRNAが分解される現象である．この現象を利用して人工的に二本鎖RNAを導入することにより，任意の遺伝子の発現を抑制することができるため，疾患原因遺伝子などの発現を標的とした治療にRNA干渉法が使用できると考えられている．しかし，この治療法を実現するには2つの大きな課題が残っている．1つは，small interfering RNA（siRNA）のデリバリー法の問題で，標的の細胞にどのようにして生体内で不安定なsiRNAを導入するかであり，2つ目はsiRNAを合成するコストが高価であることである．われわれは最初の課題に取り組み，コラーゲンを利用したsiRNAのデリバリー法について検討をしてきた．特に，慢性筋委縮疾患である筋ジストロフィーなどの治療を例として，筋ジストロフィーモデル雄性マウス咬筋に対して骨格筋形成抑制遺伝子マイオスタチンのsiRNAとアテロコラーゲンあるいは合成コラーゲンの複合体を局所投与し，咬筋におけるRNA干渉効果を検討してきた．また全身投与することによって咬筋だけでなく，前頸骨筋でのRNA干渉効果を検討し，機能的解析を行ってきた．臨床応用を考慮に入れ，siRNAとアテロコラーゲンおよび特殊加工コラーゲン複合体の研究についての研究成果について紹介する．

1．序　論

1998年にFireらは線虫の一種である*Caenorhabditis elegans*(*C.elegans*)を用いて，RNA干渉(RNA interference (RNAi))という現象を発見した[1]．この現象は，その後，ヒトに至るまで多くの生物が共通に持つ現象であることがわかった[2]．特に，siRNA（small interfering RNA）と呼ばれる21-23個の塩基からなる短い3'突出型二本鎖RNAがその主役であり，siRNAがいくつかの蛋白質複合体に結合し，相補的な配列を持つmRNAを分解することがわかった[3]．2001年には哺乳類の細胞でsiRNAを導入することで，それまで問題となってきた二本鎖RNA依存性の免疫応答反応を回避することができることがわかった．これにより，遺伝子異常が原因の疾患に対するRNA干渉治療が可能であると考えられ，応用への期待が高まってきた．2006年には，アンドリュー・ファイアーとクレイグ・メローはRNAi発見の功績によりノーベル生理学・医学賞を受賞した．

RNA干渉を利用した治療を考える場合に，2つの大きな壁が存在している．1つは，siRNAのデリバリーの問題で，2つ目は，siRNAの合成費用が高いことである．2つ目の問題については，核酸合成に関する画期的な方法が開発されるか，RNA合成酵素を利用した方法の開発が必要である．一方，最初の問題については，多くの研究者が研究しており，次々と新しい方法が提案されている[4-8]．我々はRNA干渉のための新規なsiRNAのデリバリー法として，コラーゲンに着目して研究を行っている．

これまでの研究経過を簡単に紹介する．通常，遺伝子の機能阻害（ノックアウト）実験を行うためには，染色体上の遺伝子に突然変異を導入することで行われてきた．そのためには，マウスなどの動物の遺伝子操作が必要であり，非常に時間のかかる実験である．しかし，RNA干渉法を用いた遺伝子の発現低下（ノックダウン）実験は，比較的簡単で，塩基配列さえ知ることができれば合成したsiRNAを導入することで結果を得ることができる．もちろん，ノックアウトとノックダウンでは得られる結果はまったく同じではないが，ゲノムプロジェクトによって全塩基配列を知ることのできる生物種では，遺伝子発現のノックダウンにより遺伝子の機能解析の速度を上げることが可能となる．さらに，ヒト疾患の治療を考えた場合，事実上ノックアウト法の使用は困難な治療であることから，ノックダウン法しか実質的には使用できないと考えられる．

森山啓司と野地澄晴のグループは，筋肉の形成を抑制する因子であるマイオスタチンの研究を行い，マイオスタチンの発現が抑制されたトランスジェニックマウスを用いて，筋肉が過剰に形成されることを示してきた[9]．また，マイオスタチンの発現抑制により，筋ジストロ

フィーのモデルトランスジェニックマウスにおいて，筋肉の機能が回復することを示してきた[10]．

そこで，現実的な治療方法と臨床応用のための研究として，マイオスタチンの発現抑制をRNA干渉法により行う方法について検討を行ってきた．このRNA干渉治療法では，マイオスタチンのmRNAの一部に相補的な21から25塩基配列を持つsiRNAを生体内に導入し，遺伝子の発現を抑制することを試みた．siRNAを非侵襲的かつ安全に臨床応用に用いる方法は，現在までに様々に開発されてきているが，我々は比較的処理が簡単な，アテロコラーゲン（ATCOL）（高研（株））を用いたsiRNA導入キットを用いてまず検討を行った．

次に臨床応用でのコスト面の問題点を改善する事を目的に，RNA干渉のための新規なsiRNAのデリバリー法としてATCOLの代替となり得る安価で安全性のある特殊加工コラーゲン（SYCOL）をsiRNAの導入試薬として使用してRNAi効果の検討を行った．

具体的には，1）マウス骨格筋にマイオスタチン遺伝子に対するsiRNA（*Mst*-siRNA）とATCOLの複合体を投与し，RNAi効果を検討した[11]．2）SYCOLの開発を行い，in vivo，in vitro，siRNAのRNaseによる分解阻害でATCOLとSYCOLの比較検討を行った[12]．これらの研究について紹介する．

2．研究方法について

1）（1）24～28週齢の野生型（C57BL/6）雄性マウスの右側咬筋と大腿二頭筋に*Mst*-siRNAとATCOL複合体の局所投与を行い，2週間後に咬筋と大腿二頭筋を摘出し，その筋重量を測定するとともに，形態学的ならびに組織学的解析を実施した．なお，同一個体の左側咬筋および大腿二頭筋を対照側としてスクランブルsiRNA（scr-siRNA）とATCOL複合体を投与し，*Mst*-siRNA導入を行った実験側との比較を行った．若いマウスについては，Mstの産生が少なく，効果はほとんど観察されなかった．

（2）24～28週齢の野生型（C57BL/6）雄性マウスに*Mst*-siRNAとATCOL複合体の全身投与を2週間の間に4回行い，最終投与から1週間の待機期間の後に大腿筋を摘出し，その筋重量を測定するとともに，形態学的ならびに組織学的解析を実施した．

（3）24～28週齢のDuchenne型筋ジストロフィーモデル動物である*mdx*マウスの雄を用いて右側咬筋に*Mst*-siRNAとATCOL複合体の局所投与を行い，2週間後に咬筋を摘出し，その筋重量を測定するとともに，形態学的ならびに組織学的解析を実施した．なお，同一個体の左側咬筋を対照側としてscr-siRNAとATCOL複合体を投与し，比較した．

2）（1）siRNAと特殊加工コラーゲン（SYCOL）の複合体にRNaseを接触させ，siRNAが完全に分解するまでの時間を計測し，RNaseプロテクション能力をATCOLと比較，検討した．

（2）ルシフェラーゼを恒常発現するB16-F10-luc-G5細胞にルシフェラーゼに対するsiRNA（*Luc*-siRNA）とSYCOLの複合体によってトランスフェクションを行い，RNAi効力による定量的なルシフェラーゼ発現量現象を測定した．

（3）1）（1）と同様に24～28週齢の野生型（C57BL/6）雄性マウスの右側咬筋に*Mst*-siRNAとSYCOLまたはATCOL複合体の局所投与を行い，2週間後に咬筋を摘出し，その筋重量を測定するとともに，形態学的ならびに組織学的解析を実施し，SYCOLとATCOLのRNAi効力を比較検討した．

（4）ヌードマウスを用い，右目眼窩底静脈からルシフェラーゼを恒常発現するガン細胞のB16-F10-luc-G5細胞を血流に流し全身転移させた．7日後，全身転移したB16-F10-luc-G5細胞のルシフェラーゼの発現を左目眼窩底静脈から*Luc*-siRNAとSYCOLまたはATCOLの複合体を全身投与することでSYCOLの全身投与でのRNAi効力を検討した．

3．RNA干渉法による筋肉治療のための基礎実験について

1）（1）マウス咬筋ならびに大腿二頭筋への*Mst*-siRNA/アテロコラーゲン複合体の局所投与実験の結果は下記のように報告されている[11]．

マウス咬筋の肉眼的所見では，*Mst*-siRNAを導入していない右側咬筋および大腿二頭筋（対照側）と比較して*Mst*-siRNAを導入した左側同部位では著明な骨格筋増大が認められた（Fig. 1 a）．また，その骨格筋の重量測定を行ったところ，*Mst*-siRNAを導入した咬筋および大腿二頭筋の骨格筋重量は対照側に比べ，いずれも有意に増加していた（Fig. 1 b）．組織学的検討を行うために上記同部位の骨格筋組織にて凍結切片を作成し，HE染色を行ったところ，対照群に比べ*Mst*-siRNAを導入した咬筋の最大直径部における筋線維は有意に肥大傾向を示した（Fig. 1 d, e）．また，咬筋におけるマイオスタチンの発現をウエスタンブロット法にて解析したところ，対照側と比較して*Mst*-siRNAを導入した咬筋では顕著なマイオスタチンの発現抑制が認められた（Fig. 1 c）．

（2）マウスへの*Mst*-siRNA/アテロコラーゲン複合体の全身投与実験については，下記のように

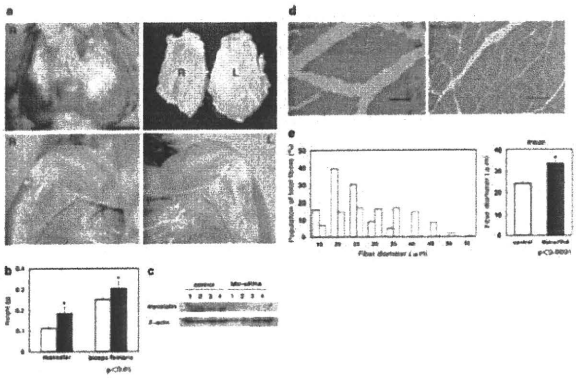

Fig. 1

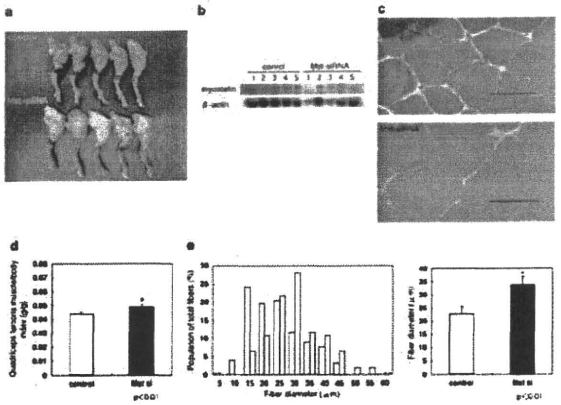

Fig. 2

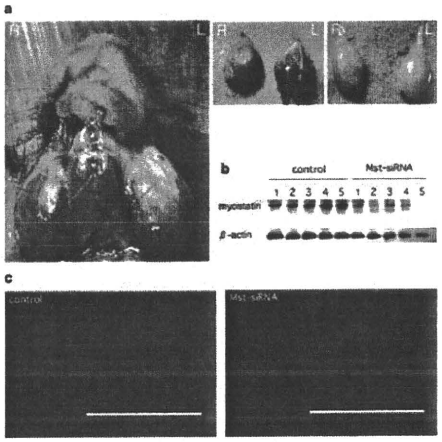

Fig. 3

報告されている[11].

マウス大腿二頭筋の肉眼所見では*Mst*-siRNAを導入していない対照群と比較して，*Mst*-siRNAを導入した実験群での著明な筋増大が見られた（Fig. 2 a），筋重量についても*Mst*-siRNA導入群で有意に増加していた（Fig. 2 d）．局所投与時と同様，組織学的検討のためにHE染色を行ったところ，対照群に比べ，*Mst*-siRNAを導入した咬筋の最大直径部における筋線維の太さを計測したところ，有意に肥大傾向を示した（Fig. 2 c，e）．大腿二頭筋におけるマイオスタチンの発現をウエスタンブロット法にて解析したところ，対照群と比較して*Mst*-siRNAを導入した実験群の大腿二頭筋では顕著なマイオスタチンの発現抑制が認められた（Fig. 2 b）．

（3）*mdx*マウス咬筋への*Mst*-siRNA/アテロコラーゲン複合体の局所投与実験の結果は，RNA干渉治療の可能性を示唆するものであった[11].

マウス咬合筋の肉眼所見では，*Mst*-siRNAを導入していない対照側と比較して，*Mst*-siRNAを導入した実験側での著明な筋増大が見られた

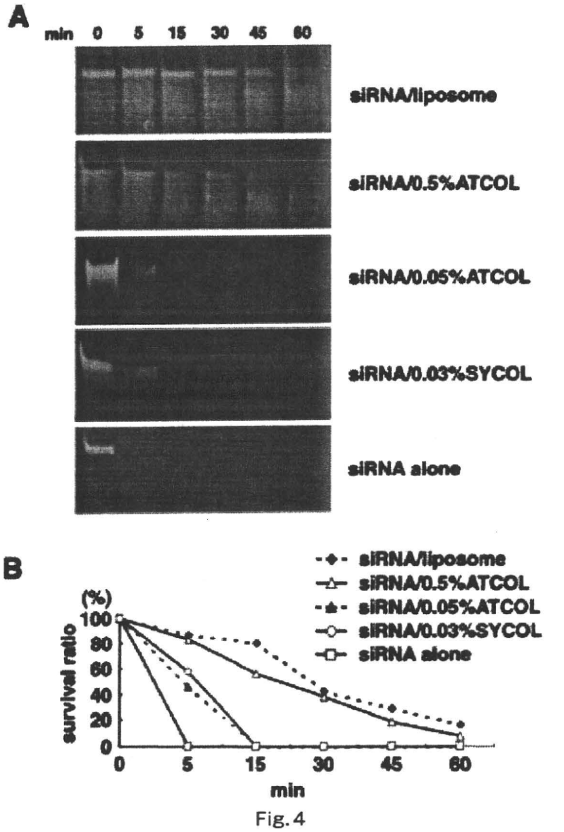

Fig. 4

(Fig. 3 a)．組織学的検討の為，凍結切片に対して抗ラミニン-α抗体を用いた蛍光免疫染色を行ったところ，筋細胞壁が染色され，対照側と比較して*Mst*-siRNA導入した実験側での筋繊維直径の増大が明らかとなった（Fig. 3 c）．また，咬筋におけるマイオスタチンの発現をウエスタンブロット法にて解析したところ，対照側と比較して*Mst*-siRNAを導入した咬筋では顕著なマイオスタチンの発現抑制が認められた（Fig. 3 b）．

2）（1）RNaseからのプロテクションアッセイの結果について[12]

siRNA/リポソーム，0.5％ATCOL，0.05％ATCOL，0.03％SYCOL複合体でRNaseからのプロテクションアッセイを行った結果，リポソームと0.5％ATCOLは同等の結果，0.05％ATCOLは0.03％SYCOLと同等の結果となった．（Fig.4）

（2）in vitroでのsiRNA/SYCOLのトランスフェクション実験について[12]

siRNA/リポソーム，ATCOL，SYCOL複合体でB16-F10-luc-G5細胞のルシフェラーゼを*Luc*-siRNAで抑制した結果，リポソーム，ATCOL，SYCOLともに同等のノックダウン結果となった．（Fig.5）

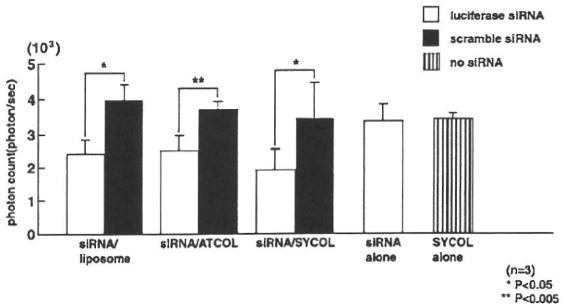

Fig.5

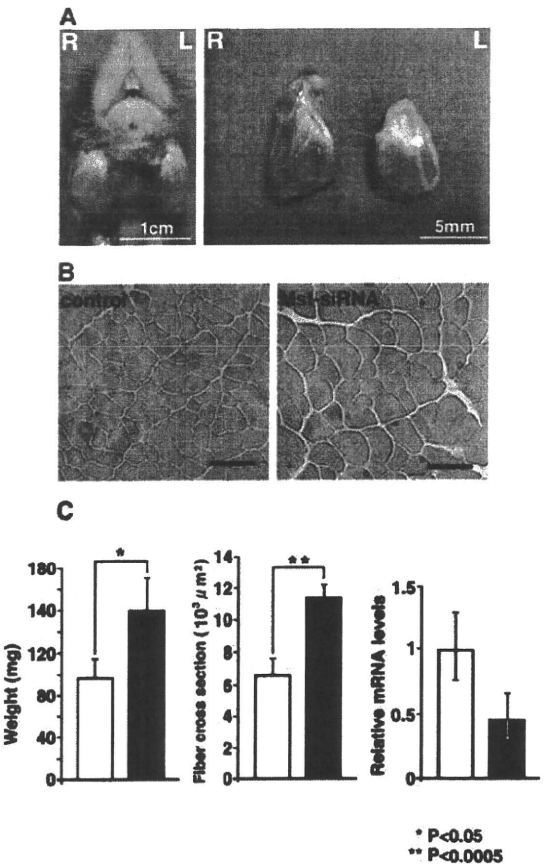

Fig.6

（3）in vivoでのsiRNA/SYCOL局所投与実験について[12]

SYCOLを用いて*Mst*-siRNAをマウス咬筋に局所投与し，その影響を調べた結果，ATCOLと同様に一度投与しただけで，2週間後には肉眼的に筋肉の増大を確認できた．*Mst*-siRNAとSYCOLの複合体投与の右側咬筋は，対照側と比較して筋重量，筋線維断面積ともに有意に増加し，mRNAの発現も有意に減少していた（Fig.6）．また，SYCOLとATCOLのmRNAサイレンシング能は同等の結果となった（Fig.7）．

（4）in vivoでのsiRNA/SYCOL全身投与実験について[12]

全身でのsiRNA/SYCOLおよびATCOLのRNAi効力を検証するためにヌードマウスに全身転移させたルシフェラーゼ発現メラノーマ細胞を*Luc*-siRNAでノックダウンし，バイオイメージングIVISで撮影した結果（Fig.8 A），ATCOLは腹部のルシフェラーゼの発現も抑制したが（Fig.8 B），SYCOLは投与した付近の発現のみを抑制していた（Fig.8 C）．

4．RNA干渉法による筋肉治療は可能であろう

近年，核酸医薬，特にsiRNAのデリバリーシステムの開発が進められているが[4-8]，血中あるいは組織中においてsiRNAの安定化は困難だと考えられてきた．今回の実験でコラーゲンを基材としたトランスフェクション試薬の咬筋および大腿二頭筋への局所投与，全身投与は1週間を超える長期間でのRNAiの効力を発揮することが認められた．また，Duchenne型筋ジストロフィーモデルマウスの*mdx*マウスへの*Mst*-siRNAの局所投与においては筋肉萎縮の回復が認められた．

また，新規siRNAトランスフェクション試薬であるSYCOLはin vitro，in vivo局所投与でATCOLと同等の

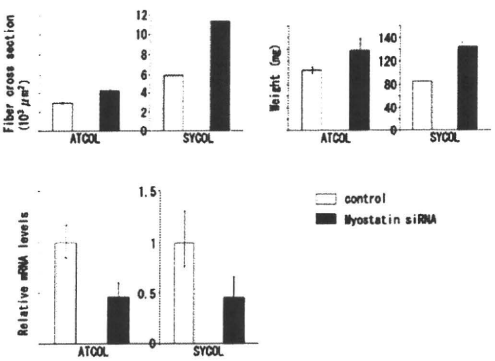

Fig.7

効力を確認することができた．しかしながらSYCOLのin vivo全身投与に関してはこれからの課題である．今後このような技術が直接成体に対して応用できる新たな治療法として進歩し，非侵襲的かつ安全に行うことが可能となれば，骨格筋異常を伴う疾患を持つ患者だけでなく様々な疾患に対するRNAi創薬の可能性がますます広がるものと期待される．

5．結論

ATCOLおよびSYCOLと*Mst*-siRNA複合体の局所導入は，筋肉内に発現するマイオスタチン遺伝子を特異的に抑制し，咬筋形成に影響を及ぼすことが示された．また，ATCOLと*Mst*-siRNA複合体の全身投与において大腿二頭筋の肥大を示したことから，骨格筋形成量の制御法として有効であることがわかった．また，臨床応用で筋肉以外の部位のガン細胞でATCOLおよびSYCOLとsiRNA複合体の効力を検討した結果，同様にRNAi効力があることが認められ，RNAi治療薬が幅広く疾患に応用できる可能性が示唆された．

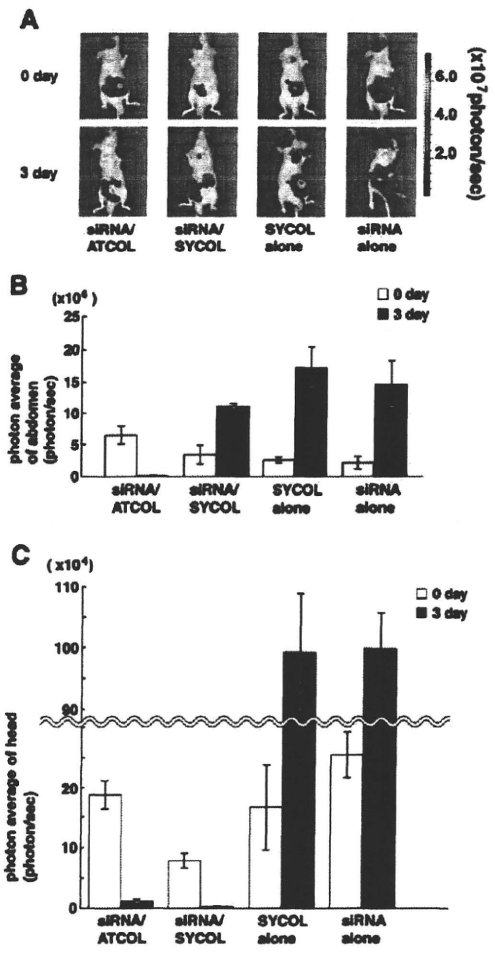

Fig. 8

1．Fire, A., Xu, S., Montgomery, M. K., Kostas, S. A., Driver, S. E., and Mello, C. C. 1998. Potent and specific genetic interference by double-stranded RNA in Caenorhabditis elegans. *Nature* 391：806-811.

2．Bernstein, E., Caudy, A.A., Hammond, S.M., and Hannon, G.J. 2001. Role for a bidentate ribonuclease in the initiation step of RNA interference. *Nature* 409：363-366.

3．Elbashir, S.M., Harborth, J., Lendeckel, W., Yalcin, A., Weber, K., and Tuschl, T. 2001. Duplexes of 21-nucleotide RNAs mediate RNA interference in cultured mammalian cells. *Nature* 411：494-498.

4．Kim, S.S., Garg, H., Joshi, A., and Manjunath, N. 2009. Strategies for targeted nonviral delivery of siRNAs in vivo. *Trends Mol Med* 15：491-500.

5．Kim, W.J., and Kim, S.W. 2009. Efficient siRNA delivery with non-viral polymeric vehicles. *Pharm Res* 26：657-666.

6．Minakuchi, Y., Takeshita, F., Kosaka, N., Sasaki, H., Yamamoto, Y., Kouno, M., Honma, K., Nagahara, S., Hanai, K., Sano, A., et al. 2004. Atelocollagen-mediated synthetic small interfering RNA delivery for effective gene silencing in vitro and in vivo. *Nucleic Acids Res* 32：e109.

7．Dykxhoorn, D.M., and Lieberman, J. 2006. Knocking down disease with siRNAs. *Cell* 126：231-235.

8．Xie, F.Y., Woodle, M.C., and Lu, P.Y. 2006. Harnessing in vivo siRNA delivery for drug discovery and therapeutic development. *Drug Discov Today* 11：67-73.

9．Nishi, M., Yasue, A., Nishimatu, S., Nohno, T., Yamaoka, T., Itakura, M., Moriyama, K., Ohuchi, H., and Noji, S. 2002. A missense mutant myostatin causes hyperplasia without hypertrophy in the mouse muscle. *Biochem Biophys Res Commun* 293：247-251.

10．Ohsawa, Y., Hagiwara, H., Nakatani, M., Yasue, A., Moriyama, K., Murakami, T., Tsuchida, K., Noji, S., and Sunada, Y. 2006. Muscular atrophy of caveolin-3-deficient mice is rescued by myostatin inhibition. *J Clin Invest* 116：2924-2934.

11．Kinouchi, N., Ohsawa, Y., Ishimaru, N., Ohuchi, H., Sunada, Y., Hayashi, Y., Tanimoto, Y., Moriyama, K., and Noji, S. 2008. Atelocollagen-mediated local and systemic applications of myostatin-targeting siRNA increase skeletal muscle mass. *Gene Ther* 15：1126-1130.

12．Adachi, T., Kawakami, E., Ishimaru, N., Ochiya, T., Hayashi, Y., Ohuchi, H., Tanihara, M., Tanaka, E., and Noji, S. 2010. Delivery of small interfering RNA with a synthetic collagen poly (Pro-Hyp-Gly) for gene silencing in vitro and in vivo. *Dev Growth Differ* 52：8.

Antisense PMO Found in Dystrophic Dog Model Was Effective in Cells from Exon 7-Deleted DMD Patient

Takashi Saito[1,2], Akinori Nakamura[1], Yoshitsugu Aoki[1], Toshifumi Yokota[3], Takashi Okada[1], Makiko Osawa[2], Shin'ichi Takeda[1]*

1 Department of Molecular Therapy, National Institute of Neuroscience, National Center of Neurology and Psychiatry, Kodaira, Tokyo, Japan, 2 Department of Pediatrics, School of Medicine, Tokyo Women's Medical University, Shinjuku, Tokyo, Japan, 3 Research Center for Genetic Medicine, Children's National Medical Center, Washington, District of Columbia, United States of America

Abstract

Background: Antisense oligonucleotide-induced exon skipping is a promising approach for treatment of Duchenne muscular dystrophy (DMD). We have systemically administered an antisense phosphorodiamidate morpholino oligomer (PMO) targeting dystrophin exons 6 and 8 to a dog with canine X-linked muscular dystrophy in Japan ($CXMD_J$) lacking exon 7 and achieved recovery of dystrophin in skeletal muscle. To date, however, antisense chemical compounds used in DMD animal models have not been directly applied to a DMD patient having the same type of exon deletion. We recently identified a DMD patient with an exon 7 deletion and tried direct translation of the antisense PMO used in dog models to the DMD patient's cells.

Methodology/Principal Findings: We converted fibroblasts of $CXMD_J$ and the DMD patient to myotubes by FACS-aided MyoD transduction. Antisense PMOs targeting identical regions of dog and human dystrophin exons 6 and 8 were designed. These antisense PMOs were mixed and administered as a cocktail to either dog or human cells *in vitro*. In the $CXMD_J$ and human DMD cells, we observed a similar efficacy of skipping of exons 6 and 8 and a similar extent of dystrophin protein recovery. The accompanying skipping of exon 9, which did not alter the reading frame, was different between cells of these two species.

Conclusion/Significance: Antisense PMOs, the effectiveness of which has been demonstrated in a dog model, achieved multi-exon skipping of dystrophin gene on the FACS-aided MyoD-transduced fibroblasts from an exon 7-deleted DMD patient, suggesting the feasibility of systemic multi-exon skipping in humans.

Citation: Saito T, Nakamura A, Aoki Y, Yokota T, Okada T, et al. (2010) Antisense PMO Found in Dystrophic Dog Model Was Effective in Cells from Exon 7-Deleted DMD Patient. PLoS ONE 5(8): e12239. doi:10.1371/journal.pone.0012239

Editor: Antoni L. Andreu, Hospital Vall d'Hebron, Spain

Received May 7, 2010; **Accepted** July 21, 2010; **Published** August 18, 2010

Funding: This work was supported by the Health and Labour Sciences Research Grants for Translational Research from the Ministry of Health, Labour and Welfare of Japan (H19-Translational Research-003, H21-Translational Research-011, H21-Clinical Research-011). The funders had no role in study design, data collection and analysis, decision to publish, or preparation of the manuscript.

Competing Interests: The authors have declared that no competing interests exist.

* E-mail: takeda@ncnp.go.jp

Introduction

Antisense oligonucleotides (AON) have been reported to modulate splicing of pre-mRNA transcribed from mutated genes and to restore a normal reading frame in several diseases. Duchenne muscular dystrophy (DMD), a degenerative muscle disorder caused mainly by nonsense or frame-shift mutations of the dystrophin gene, is one of the diseases that could be treated by AON-mediated exon skipping. Previously reported studies were conducted *in vitro*, in animal models, and as patient intervention studies, and they showed restorations of the reading frame in dystrophin mRNA and recoveries of dystrophin protein expression [1,2,3]. Among the several AON chemistries that have been introduced thus far, a phosphorodiamidate morpholino oligomer (PMO) and 2'-O-methyl phosphorothioate (2'OMe) oligomer are promising candidates owing to their stabilities and efficacies, and they are now undergoing phase I-II clinical trials in the United Kingdom and the Netherlands, respectively [4,5]. The AON-mediated exon skipping is already in a late early stage of clinical application; therefore, it is rational to translate pre-clinical animal model knowledge into a patient-based study.

We have previously reported that the systemic administration of an antisense PMO for canine X-linked muscular dystrophy in Japan ($CXMD_J$) achieved restoration of dystrophin and amelioration of symptoms [6]. $CXMD_J$ harbors a splice site mutation within the splice acceptor site of intron 6 of the dystrophin gene. The mutation disrupts the splicing of exon 7, and thus the dystrophin mRNA lacks exon 7 [7]. In $CXMD_J$, multiple skipping of exons 6 and 8 restores the reading frame, and the multi-exon skipping approach is expected to expand the number of DMD cases potentially treatable by exon skipping [8]. $CXMD_J$ is an ideal model of multi-exon skipping, and we hope to translate the results to human patients. However, in the road to ongoing clinical trials, *in vitro* assays on patient cells are indispensable.

To date, antisense sequences used for exon skipping in DMD animal models have not been directly applied to a DMD patient having the same type of exon deletion. We identified an exon 7-deleted patient (referred to as DMD 8772) and tried direct

translation of the antisense PMO design from a DMD dog model to the DMD patient. We tried *in vitro* multi-exon skipping with the same antisense PMO that was used in $CXMD_J$ in the patient's cells before attempting delivery of the PMO into the patient.

Which cells should be used for *in vitro* dystrophin exon skipping is controversial. Myoblasts are usually employed simply because they express enough dystrophin as mRNA and protein, but collecting them requires an invasive muscle biopsy. In cases where myoblasts were not available, it had been reported that the dystrophin mRNA was detected in lymphocytes and fibroblasts by nested RT-PCR. Some studies actually demonstrated the success of exon skipping in mRNA of lymphoblastoid cells and fibroblasts [9,10], but the restoration of dystrophin protein could not be analyzed in these cells because their transcripts were illegitimate and too low to be translated into gene products [11]. As another alternative, fibroblasts are converted to myotubes by MyoD transduction [4,12,13]. Transduced cells express dystrophin mRNA and protein, but achievement of sufficient protein expression is challenging [14,15,16]. In this study, we addressed this issue by introducing a retroviral vector co-expressing MyoD and green fluorescent protein (GFP) and flow cytometry, and then quantified the dystrophin expression of the cells to evaluate the feasibility of exon skipping.

We first report multiple skipping of dystrophin exons 6 and 8 in the DMD patient's cells and translation of the unified antisense PMO design from a DMD dog model to a human based on the MyoD-transduction method utilizing flow cytometry.

Results

Mutation analysis of DMD 8772

DMD 8772, a 22-year-old man, manifested severe muscle weakness, wheelchair dependency, and mild cardiac dysfunction. No evidence of dystrophin protein had been observed on a previous muscle biopsy, and the patient had been diagnosed with a frame-shift deletion of dystrophin exon 7 by multiplex ligation-dependent probe amplification (MLPA) analysis. The deletion of exon 7 leads to a premature translation termination at exon 8. The deletion of exon 9 is known as a common splice variant maintaining the reading frame in dogs and humans [17,18] (**Figure 1A**). RT-PCR analysis of dystrophin mRNA using the patient's lymphocytes showed an exon 7 deletion, and direct sequence analysis of the RT-PCR products revealed a conjunction of exons 6 and 8 (**Figure 1B**). To determine the intron length, we performed a deletion breakpoint analysis. The genomic PCR roughly narrowed the breakpoint window to 2.5 kb between introns 6 and 7, then primer walking sequence analysis revealed the 50.4 kb deletion (Vega v35 chromosome X 32771568 to 32821979) [13] and the breakpoint accompanying an insertion of 13 bases of unknown origin (**Figure 1C**).

Myogenic conversion of fibroblasts by MyoD transduction and selection of appropriate cell lineage for exon skipping

We prepared lymphoblastoid cells, fibroblasts, and MyoD-transduced fibroblasts from DMD 8772 and assessed the feasibility of exon skipping in these cells. To establish MyoD-transduced fibroblasts, primary fibroblasts were transfected by a retrovirus encoding murine or human MyoD and GFP with the vesicular stomatitis virus (VSV-G) envelope through standard procedures (**Figure 2A**) [19,20]. To compare exon skipping between corresponding cells of $CXMD_J$ and DMD 8772, fibroblasts from both were converted. In addition, normal dog and human fibroblasts were also transduced for evaluation. After virus transfection, we

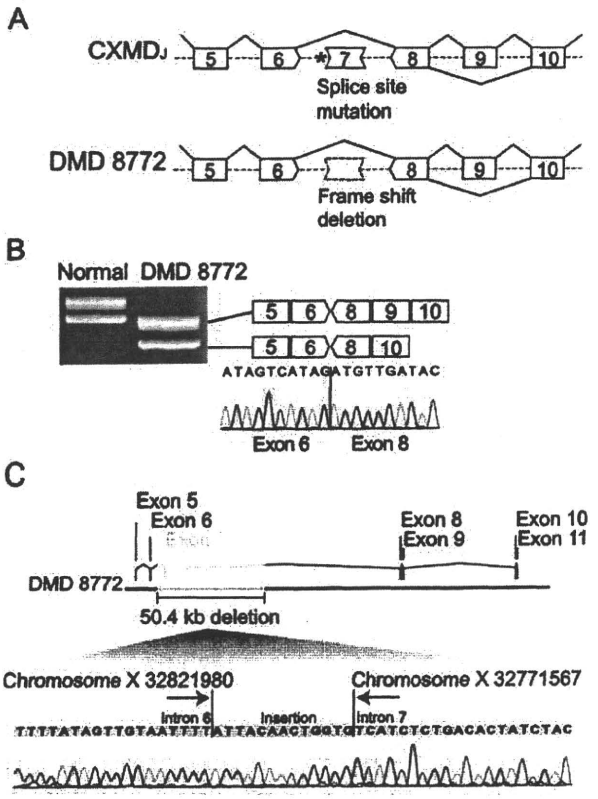

Figure 1. Mutation analysis of DMD 8772. (A) Splice-site mutation of a splice acceptor site in intron 6 (asterisk) excludes exon 7 from dog dystrophin mRNA. Frame-shift deletion of dystrophin exon 7 in DMD 8772 was diagnosed by MLPA analysis. Skipping of exon 9 is a frequent splice variant. Both ends of the schematic box of the exon represent a phase of the codon (see detail, Yokota et al. 2009). (B) RT-PCR and sequence analysis of dystrophin mRNA using normal and DMD 8772 lymphocytes. Double bands due to a splicing variant of exon 9 were observed. (C) Breakpoint analysis of DMD 8772 revealed a 50.4 kb deletion from intron 6 to intron 7, and the insertion of 13 bases of unknown origin.
doi:10.1371/journal.pone.0012239.g001

sorted GFP-positive cells by flow cytometry. The ratio of GFP-positive to -negative cells was dependent on cell lineage, and affected cells generally showed lower transfection efficiencies (**Figure 2B**). The GFP-positive cells were isolated in serum-deprived medium for myogenic differentiation and cultured for 10 to 16 days. We confirmed that the cultured cells had the morphological features of myotubes of multiple nuclei and longitudinal growth. Immunostaining analysis showed nuclear localization of MyoD and expressions of the muscle-specific proteins desmin, myosin heavy chain, and dystrophin (**Figure 2C**). Using normal dog and human fibroblasts, we performed time-course expression analyses of dystrophin mRNA by qRT-PCR and dystrophin protein by Western blot. The results showed a gradual increase in dystrophin expression. In dog cells, dystrophin became detectable on the protein level seven days after differentiation, whereas human cells required two weeks or more (**Figure 2D**). We compared the dystrophin mRNA expression of the lymphoblastoid cells, fibroblasts, and MyoD-transduced fibroblasts from DMD 8772. The MyoD-transduced fibroblasts showed remarkable expression compared with the other cells (**Figure 2E**). We tried exon skipping in lymphoblastoid cells, fibroblasts and MyoD-transduced fibroblasts, but only the MyoD-transduced

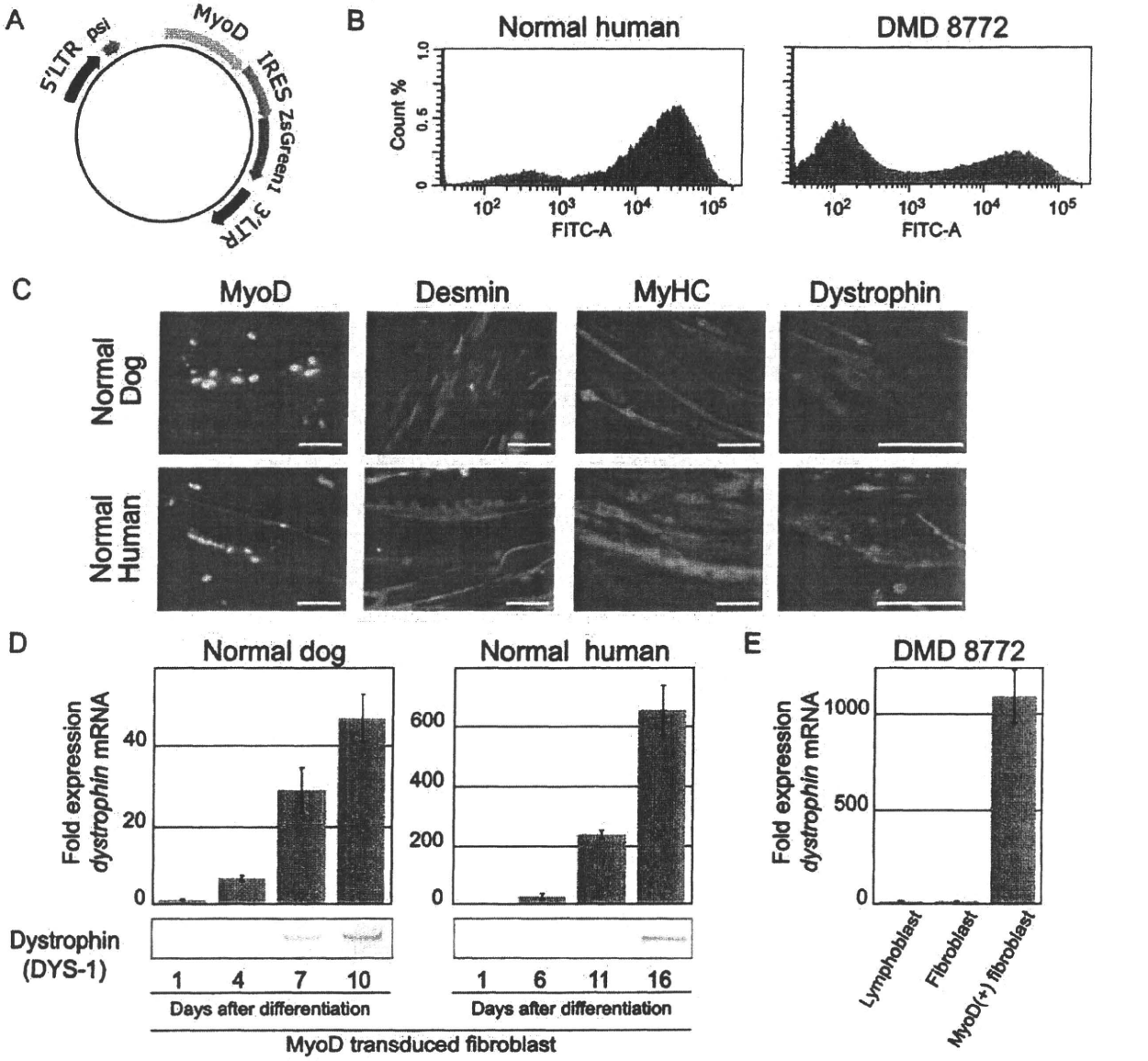

Figure 2. Myogenic conversion of fibroblasts and dystrophin expression. (A) Schematic diagram of the retroviral expression vector. (B) Histograms showing GFP fluorescence intensity compared with cell numbers of normal human and DMD 8772 MyoD-GFP-transduced fibroblasts. Both cells were analyzed five days after retroviral transfection. (C) Immunostaining of MyoD-transduced of dog and human fibroblasts after 10 and 15 days of myogenic differentiation, respectively. MyHC, myosin heavy chain. The nuclei were counter-stained with DAPI. Scale bar: 100 μm. (D) The time course of dystrophin expression in dog and human MyoD-transduced fibroblasts by qRT-PCR and immunoblotting analysis. The mRNA levels were normalized to *GAPDH* and expressed relative to the amount of the lowest one in each group. For immunoblotting, 5 μg of total protein was loaded into each lane. Error bars indicate standard deviation. (E) Determination of dystrophin mRNA expression in each cell type from DMD 8772 by qRT-PCR. MyoD-transduced fibroblasts were assayed 15 days after differentiation. Normalization and relative expression are the same as (D).
doi:10.1371/journal.pone.0012239.g002

fibroblasts yielded reproducible results. The lymphoblastoid cells and fibroblasts often failed to produce PCR products, and the skipped in-frame products were undetectable even if PCR products were generated (**data not shown**). Therefore, we used MyoD-transduced fibroblasts in the subsequent assays.

Antisense PMO sequence design

In a previous systemic dog study, we used three antisense sequences, Ex6A, Ex6B, and Ex8A, as three antisense PMO cocktails [6]. Because there were two base mismatches between dog and human Ex6B, hEx6B was newly designed on the identical region of Ex6B, modifying the mismatches of the human sequence. In the systemic study, we skipped exon 6 with a combination of Ex6A and Ex6B, and thus we tried same strategy for exon 8. We newly designed several antisense PMOs targeting exon 8 that were positioned on the identical sequence in dog and human considering the predicted *in silico* splice-enhancer motifs (**Figure 3A**). A preliminary assay of $CXMD_J$ cells showed that three sequences, Ex8G, Ex8I, and Ex8K, were effective. Therefore, the antisense combination for exon 8 contained an extra antisense sequence

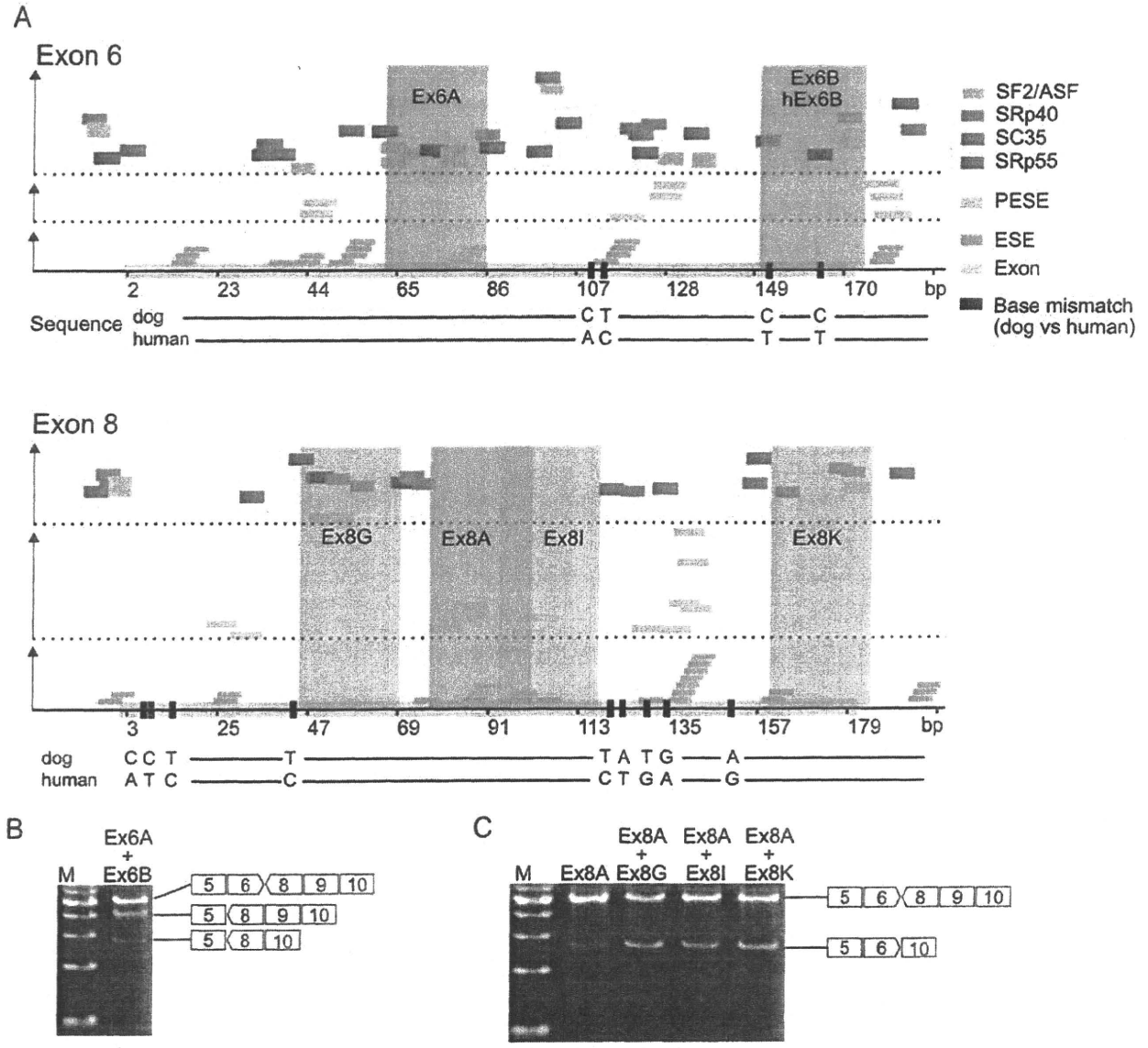

Figure 3. Design of antisense PMO sequence targeting exons 6 and 8. (A) Exonic splicing enhancer motifs predicted *in silico* based on human sequence (small coloured boxes) and positions of antisense PMOs (green and blue rectangular areas). The horizontal axis represents base positions in each exon from 5′ to 3′, and the vertical axis represents relative predicted values of the motifs. PESE: putative exonic splicing enhancer. ESE: exonic splicing enhancer. Base mismatches between dog and human (black bar) are indicated in the exon (grey box). RT-PCR of dystrophin mRNA of MyoD-transduced $CXMD_J$ fibroblasts treated with (B) a mixture of Ex6A and Ex6B and (C) only Ex8A or mixtures containing Ex8A.
doi:10.1371/journal.pone.0012239.g003

from Ex8G, Ex8I, or Ex8K in addition to that of Ex8A. The skipping efficacy of each combination was higher than that of Ex8A alone, and those of Ex8G, Ex8I, and Ex8K were comparable (**Figure 3C**).

Comparison of multiple skipping of exons 6 and 8 between $CXMD_J$ and DMD 8772 cells

The multi-exon skipping of exons 6 and 8 employed three- and four-antisense PMO cocktails. In the three-antisense PMO cocktail for dogs, Ex6A, Ex6B, and Ex8A were included, and Ex6B was replaced with hEx6B for the human. The four-antisense PMO cocktail included one of Ex8G, Ex8I, or Ex8K in addition to the three-antisense PMO cocktail (**Figure 4A**). When we transfected the three- or four-antisense PMO cocktails into the MyoD-transduced fibroblasts, we did not observe the skipped products (231 bp) of exons 6-8 on RT-PCR analyses of $CXMD_J$ but did observe the skipped products (99 bp) of exons 6-9. A sequence analysis also confirmed the concatenation of exons 5 and 10. In DMD 8772, we observed skipped products (221 bp and 92 bp, respectively) of both exons 6-8 and exons 6-9. Sequence analysis also showed that the skipped products were concatenations of exons 5 to 9 and exons 5 to 10. The four-PMO cocktails produced more in-frame products than the three-PMO cocktail, but we discerned no difference among the four PMO cocktails. This tendency was also consistent between $CXMD_J$ and DMD 8772 (**Figure 4B**). Immunostaining analysis showed partial recovery of dystrophin in the four-antisense PMO

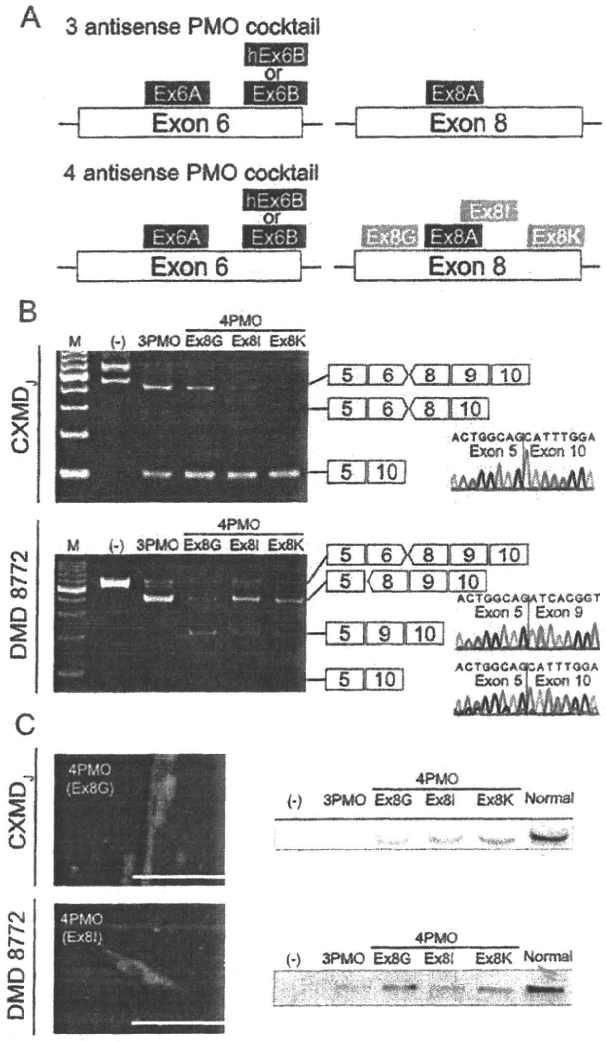

Figure 4. Multi exon skipping and recovery of dystrophin in CXMD$_J$ and DMD 8772-derived cells. (A) Schematic diagram of the three- and four-antisense PMO cocktails. For DMD 8772, Ex6B was replaced with hEx6B. In the four-antisense PMO cocktail, one additional sequence (Ex8G, Ex8I, or Ex8K) was added to the three-antisense PMO cocktail. (B) RT-PCR of dystrophin mRNA isolated from MyoD-transduced fibroblasts after treatment with the three- and four-antisense PMO cocktails. In-frame exon skipping products were 99 bp in dog and 221 bp and 92 bp in human. (C) Representative immunostaining and immunoblotting analysis of MyoD-transduced fibroblasts treated with antisense PMO cocktails. The nuclei were counterstained with DAPI. Scale bar: 100 μm. Expected molecular weights of truncated human dystrophin with exons 6–8 and exons 6–9 skipped are 18.3 kDa and 23.1 kDa, respectively, smaller than the full-length dystrophin.
doi:10.1371/journal.pone.0012239.g004

cocktail-treated cells without obvious differences between them (**Figure 4C**). Western blots of dystrophin showed products that were slightly smaller than the full-length dystrophin. In RT-PCR of DMD 8772, skipped mRNA of both exons 6-8 and 6-9 were detected; however, distinguishing the truncated dystrophins translated from these mRNA variants was impossible. Similar to the RT-PCR results, the dystrophin expression level was higher with a four-PMO cocktail than with the three-PMO cocktail. Differences between the four-PMO cocktails were also undetectable.

Discussion

In this study, we accomplished *in vitro* multi-exon skipping in a DMD patient carrying the same deletion as CXMD$_J$ by using the identical antisense PMO. We also addressed the efficient MyoD transduction of fibroblasts with FACS, and discuss the difference of the spliced exon associated with it with the frequency of alternative splicing.

FACS-aided MyoD transduction provided sufficient dystrophin expression

We evaluated the appropriateness of lymphoblastoid cells, fibroblasts, and MyoD-transduced fibroblasts as an alternative to myoblasts for exon-skipping assays. Lymphoblastoid cells and primary fibroblasts dystrophin mRNA required reamplification by nested RT-PCR [9,10], and the results were not reproducible, suggesting that low dystrophin expression may hamper reliable quantitative assessments. Only MyoD-transduced fibroblasts showed reproducible results due to their stable dystrophin expression. We employed flow cytometry for selection of MyoD-positive cells; it seems to offer several advantages against conventional drug-resistance selection. First, the transfection ratio in drug-resistance selection remains unknown until a selective drug is added. In contrast, with MyoD-transduced fibroblasts, we were able to roughly determine the ratio by fluorescence microscopy and adjust the culture scale to meet the size of the assay. Second, a low rate of myotubes formation after drug-resistance selection has been reported [21]. Our method actively selects MyoD-positive cells and enables pure clusters of MyoD-positive cells to form myotubes efficiently. MyoD transduction with GFP has been reported in several studies [22,23] but not in dystrophin exon-skipping studies. We demonstrated that it is a suitable approach for the exon-skipping assay here as well. Several studies have reported difficulties inducing dystrophin in human cells with MyoD transduction [14,15,16]. In our experience, the typical morphological features of myotubes, multiple nuclei and longitudinal cell growth, do not necessarily indicate sufficient dystrophin expression. Seeding MyoD-positive cells at high density ($>5.0\times10^4$ cells/cm^2) and incubating for longer periods (>2 weeks) were critical to induce sufficient dystrophin expression. Detachment of differentiated myotubes from culture wells was also problematic; supporting them with a coating matrix seems to promise better results.

Direct translation of antisense PMO from dog to human was feasible

We previously reported systemic multi-exon skipping in CXMD$_J$ with a 3-antisense PMO cocktail and amelioration of dystrophic pathology [6]. The effectiveness of the 3-antisense PMO cocktail was confirmed in MyoD-transduced fibroblasts derived from DMD 8772 as well. When the dog and human sequences were compared, 97% of dystrophin exon 6 and 95% of dystrophin exon 8 matched on the sequence level. This similarity enabled use of the unified antisense design methodology targeting the same sequence. We demonstrated that the identical antisense PMO sequence designed for dog and achieved multi-skipping of exons 6 and 8 in human cells. The skipping efficacies of the PMOs were indistinguishable between CXMD$_J$ and DMD 8772; the superior efficacy of the four-PMO cocktail against that of the three-PMO cocktail and the equivalent efficacies of each four-PMO cocktail were comparable. CXMD$_J$ shows more similarity in the pathogenic phenotype to human DMD than to *mdx* mice [24]. These findings imply that not only the similarity in the sequence but also the similarity in the pathogenic phenotype contributed to the comparable results.

No study has yet compared the exon skipping due to identical antisense PMOs between cells of different species carrying same exon deletion in mRNA. Recent investigations have reported a limitation in designing efficient antisenses to induce human dystrophin skipping in a mice model assay [25]; however, we confirmed the feasibility of direct translation of an antisense PMO from a DMD dog model to a DMD patient, at least *in vitro*, for the first time.

The four-antisense PMO cocktail, the addition of a fourth antisense sequence to the three-antisense PMO cocktail, increased the efficiency of skipping as previously reported [26,27]. The effectiveness of the four-antisense PMO cocktails, however, must be evaluated *in vivo*, and we are planning systemic treatment of $CXMD_J$ with them. Our results underscore the usefulness of $CXMD_J$ as a DMD model for translational research and advance the prospect that systemic treatment of the DMD patient by multi-exon skipping is possible.

Mode of exon 9 skipping might be affected by frequency of alternative splicing

With the antisense PMO targeting exons 6 and 8, exon 9 was always skipped in $CXMD_J$, although it was only partially skipped in DMD 8772. Two possibilities were considered to explain the difference: (1) the effects of the shortened introns 6 and 7 due to the deletion around exon 7 in DMD 8772 (**Figure 5**), and (2) the different frequencies of alternative splicing of exon 9. For the former case, we tried exon 8 skipping using a combination of Ex8A and Ex8G in normal and affected human MyoD-transduced fibroblasts, and found that the skipping of exon 8 and exons 8/9 happened simultaneously (**Figure S1**). Therefore, it is unlikely that the intron length affects the difference. In the latter case, the untreated MyoD-transduced fibroblasts from $CXMD_J$ clearly showed one normal and one alternative transcript; on the other hand, the untreated sample from DMD 8772 showed only a normal transcript, suggesting that the frequency of alternative splicing of exon 9 is an underlying factor in the difference. It was reported that an antisense oligonucleotide targeting exon 8 facilitates the skipping of exon 9 as well as exon 8 by effecting the concatenation of exons 8 and 9 in human and dog cells [28].

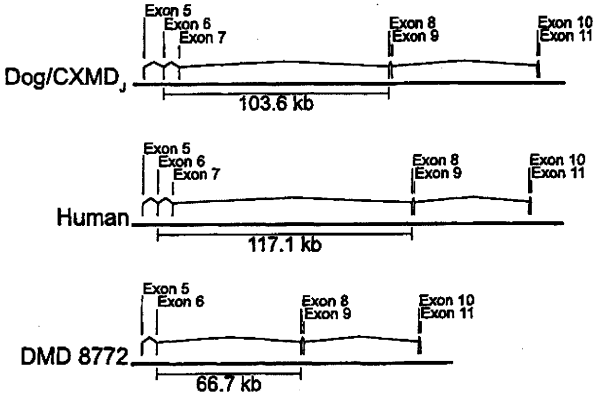

Figure 5. Location of dystrophin exons 5 to 11 in the genome. Distances from dystrophin exon 6 to exon 8 are indicated based on the GenBank reference sequences of *Canis familiaris* chromosome X genomic contig, whole genome shotgun sequence (NW_879562.1) and *Homo sapiens* 211000035840903 genomic scaffold, whole genome shotgun sequence (CH471074.1).
doi:10.1371/journal.pone.0012239.g005

These findings were observed in myoblasts but not in MyoD-tansduced fibroblasts [29,30,31]. As is well known, the mode of alternative splicing differs among various tissues [32,33], and our MyoD-transduced fibroblasts might have characteristics that are incompatible with the alternative splicing of exon 9.

In summary, MyoD transduction of fibroblasts with the help of FACS may be practical for exon skipping assays, and the direct translation of an antisense PMO from a DMD dog model to a DMD patient was feasible *in vitro*, suggesting that the animal model-based antisense PMO for multiple skipping could be effective for humans as well.

Materials and Methods

Ethics Statement

The patient samples were collected and used with the approval of the Ethics Committee of the National Center of Neurology and Psychiatry, approval ID: 20-4-6. Written informed consent was obtained from the donor. The dog study was approved by the Ethics Committee for the Treatment of Middle-sized Laboratory Animals of the National Center of Neurology and Psychiatry, approval ID: 20-05.

Cell culture

Dog primary myoblasts and fibroblasts were obtained from muscle specimens of normal and affected neonatal dogs of the $CXMD_J$ colony using a standard pre-plating technique. Primary fibroblasts of the DMD patient (DMD 8772) were obtained from skin explants and peripheral blood lymphocytes using Lymphocyte Separating Medium (PAN Biotech GmbH, Aidenbach, Germany). Lymphoblastoid cell lines were established by transformation with Epstein-Barr virus. The normal human fibroblast cell line TIG-119 was obtained from the Health Science Research Resource Bank (Osaka, Japan). Fibroblasts were cultured in 20% or 10% growth medium containing DMEM/F-12 1:1 (Invitrogen, San Diego, CA, USA), 20% or 10% fetal bovine serum, and 1% penicillin/streptomycin. For differentiation to myotubes, FACS-sorted MyoD-transduced fibroblasts were cultured in 2% differentiation medium containing DMEM/F-12 1:1, 2% horse serum, ITS Liquid Media Supplement (Sigma-Aldrich, St. Louis, MO, USA), and 1% penicillin/streptomycin.

Genomic mutation analysis

The dystrophin exon 7-deletion of DMD 8772 had been identified previously by MLPA. For breakpoint detection, lymphocyte genomic DNA was used as a template. Seven pairs of intron-spanning primers, positioned in the intron 6/7, were designed to yield 150-600 bp PCR products. A failure of PCR indicated deletions spanning the primer annealing sites. Four of seven primer pairs showed no amplification, suggesting that the deletion was more than 3.5 kb and less than 64.4 kb. Additionally, two intron 6 sense-primers and eight intron 7 antisense-primers were designed. Each primer pair was placed by flanking the breakpoint and expected to yield PCR products within the range of 4–64 kb. Primer sequences are available on request. PCR was performed using Phusion Hot Start High-Fidelity DNA Polymerase (Finnzymes, Keilaranta, Finland), and the cycling program was set to yield 16 kb products with a program of 35 cycles of 98°C for 10 sec, 60°C for 30 sec, and 72°C for 450 sec. Failure of PCR indicated products of more than 16 kb in size or the deletion of annealing sites. The breakpoint region was thus narrowed down to 2.5 kb, then primer walk sequencing was performed (Operon Biotechnologies, Tokyo, Japan).

MyoD transduction and cell sorting by FACS

The coding sequences of mouse *Myod1* (CCDS 21277.1) and human *MYOD1* (CCDS 7826.1) were derived from the Consensus CDS database [34]. The sequences were synthesized and cloned into a pUC57 vector (GenScript, Piscataway, NJ, USA). We subcloned it into a pRetroX-IRES-ZsGreen1 expression vector (Clontech, Mountain View, CA, USA). The expression vector, a pVSV-G envelope vector, and a gap-pol expression vector were co-transfected into a 293T packaging cell line using the standard calcium phosphate method. After 48–72 h incubation, the viral supernatant was collected and stored at −80°C. For retroviral transduction, the fibroblasts were harvested at 70–80% confluence in a T225 flask, and 2.5 ml thawed retroviral stock was added to 35 ml of growth medium. We added polybrene (Sigma-Aldrich) to a final concentration of 8 μg/ml. After 48–72 h incubation at 32°C, the culture medium was replaced with fresh growth medium, the cells were incubated at 37°C 1–3 d more, until the GFP-positive cells exceeded approximately 60%. Cell sorting was performed on a FACS VantageSE or FACSAria flow cytometry system (BD Bioscience, Franklin Lakes, NJ, USA). The recovered GFP-positive cells were seeded in Matrigel (BD Bioscience)-coated well plates at density of 5×10^4 cell/cm^2. After confirmation of cell attachment, the culture medium was changed to 2% differentiation medium. We cultured MyoD-transduced fibroblasts for 10 to 16 d to differentiate to myotubes.

Antisense PMO design and transfection to cultured cells

The antisense PMO sequences Ex6A, Ex6B, and Ex8A were described in Yokota et al. [6]. In addition, extra sequences hEx6B, Ex8G, Ex8I, and Ex8K were designed and synthesized (Gene Tools, LLC, Philomath, OR, USA). We used the Human Splicing Finder for *in silico* prediction of the splice-enhancer motifs [35]. All sequences are shown in **Table S1**. We transfected the antisense PMOs into myotubes differentiated from MyoD-transduced fibroblasts with a transfection agent, Endo-Porter (Gene Tools). In the 2% differentiation medium, the final concentration of the antisense PMO was 10 μM for a single sequence, 20 μM for two sequences, and a total of 30 μM for three or four sequences. A final concentration of Endo-Porter was 6 μM. After 48–72 h incubation with the PMO, the medium was changed to a fresh culture medium free of PMOs. The cells were recovered for analysis after 24–48 h in the PMO-deprived medium to allow sufficient time to translate dystrophin protein.

Quantitative RT-PCR analysis

Total RNA was extracted from MyoD-transduced fibroblasts obtained from normal subjects using Trizol (Invitrogen) at the time points specified. Total RNA (100-200 ng) was employed for cDNA synthesis using a QuantiTect Reverse Transcription Kit (Qiagen, Hilden, Germany). Quantitative real-time PCR was performed using ExTaq II SYBR (Takara, Kyoto, Japan) and a MyiQ Single-Color Real-Time PCR detection system (Bio-Rad, Hercules, CA). Primer sequences are shown in **Table S2**. Expression of dystrophin mRNA was normalized to *GAPDH* mRNA, and the time course of the increment was calculated by the delta-delta-Ct method.

RT-PCR and sequence analysis

As well as quantitative RT-PCR analysis, total RNA extraction and cDNA synthesis were performed. For myoblasts and MyoD-transduced fibroblasts, 35 cycles of denaturing at 98°C for 10 sec, annealing at 63°C for 30 sec, and extension at 72°C for 1 min were performed with ExTaq DNA polymerase (Takara). For fibroblasts and lymphoblasts, nested PCR was performed. Primer sequences are shown in **Table S3**. PCR products were electrophoresed on 1.2% SeaKem LE agarose gel (Lonza, Basel, Switzerland). The bands of interests were excised using a Wizard SV Gel and PCR Clean-Up system (Promega, Fitchburg, WI, USA), then sequenced directly or cloned into a vector using a TOPO-TA Cloning Kit (Invitrogen) with standard cloning techniques. Sequencing was performed by Fasmac Corporation (Kanagawa, Japan).

Immunostaining analysis

Cells were fixed in 3% paraformaldehyde, permeabilized in 10% Triton-X, then blocked by 10% goat serum in PBS for 1 h at room temperature. The cells were incubated with the primary antibody for 1 h at room temperature using anti-dystrophin (NCL-Dys1, diluted 1:30, Novocastra, Newcastle upon Tyne, UK), anti-myosin heavy chain (NCL-MHCf, diluted 1:30, Novocastra), anti-MyoD (NCL-MyoD1, diluted 1:30, Novocastra), or anti-desmin (NCL-DES-DERII, diluted 1:30, Novocastra). Incubation with the secondary antibody was performed for 30 min at room temperature using anti-rabbit or anti-mouse IgG (Alexa Fluor 546 highly cross-adsorbed, diluted 1:300, Invitrogen). Antibodies were diluted in Can Get Signal Immunostain A solution (Toyobo, Osaka, Japan). To visualize nuclei and enhance fluorescence signals, cells were mounted with Pro Long Gold Antifade reagent (Invitrogen).

Immunoblotting analysis

Protein was extracted from cultured cells using RIPA buffer (Thermo Fisher Scientific, Rockford, IL, USA) containing Complete Mini (Roche Applied Science, Indianapolis, IN, USA) as a protease inhibitor. Protein concentrations were determined using a BCA protein assay kit (Thermo Fisher Scientific) and equalized. After being mixed with an equal volume of EzApply sample buffer (ATTO Corporation, Tokyo, Japan), cell lysates containing equal amounts of total protein were denatured at 95°C for 5 min, electrophoresed in NuPAGE Novex Tris-Acetate Gel 3–8% (Invitrogen) at 150 V for 75 min, and transferred onto an Immobilon-P membrane (Millipore Corp., Billerica, MA, USA). Membranes were blocked for 1 h with 5% ECL Blocking agent (GE Healthcare, Buckinghamshire, UK) and probed with anti-dystrophin antibody (NCL-Dys1, diluted 1:50, Novocastra), followed by incubation with peroxidase-conjugated goat-anti-mouse IgG (Bio-Rad). An ECL Plus Western blotting system (GE Healthcare) was used to detect protein bands.

Supporting Information

Figure S1 RT-PCR of dystrophin mRNA isolated from the normal and affected human MyoD-transduced fibroblasts after the single exon 8 skipping.
Found at: doi:10.1371/journal.pone.0012239.s001 (0.30 MB PDF)

Table S1 Sequences of antisense PMO for dystrophin gene (for dog and human if not specified).
Found at: doi:10.1371/journal.pone.0012239.s002 (0.07 MB PDF)

Table S2 Sequences of qRT-PCR primers.
Found at: doi:10.1371/journal.pone.0012239.s003 (0.07 MB PDF)

Table S3 Sequences of RT-PCR primers.
Found at: doi:10.1371/journal.pone.0012239.s004 (0.07 MB PDF)

Acknowledgments

The authors thank Yu-ichi Goto (Department of Mental Retardation and Birth Defect Research, National Center of Neurology and Psychiatry), Narihiro Minami (Department of Neuromuscular Research, National Center of Neurology and Psychiatry), Hirofumi Komaki (Department of Child Neurology, National Center of Neurology and Psychiatry), Katsutoshi Yuasa (Research Institute of Pharmaceutical Sciences, Faculty of Pharmacy, Musashino University, Tokyo, Japan), and Tetsuya Nagata, Yuko Shimizu, and Satoru Masuda (Department of Molecular Therapy, National Center of Neurology and Psychiatry) for useful discussions and technical assistance.

Author Contributions

Conceived and designed the experiments: TS AN ST. Performed the experiments: TS YA. Analyzed the data: TS MO. Contributed reagents/materials/analysis tools: TY TO. Wrote the paper: TS AN ST.

References

1. Aartsma-Rus A, Bremmer-Bout M, Janson AA, den Dunnen JT, van Ommen GJ, et al. (2002) Targeted exon skipping as a potential gene correction therapy for Duchenne muscular dystrophy. Neuromuscul Disord 12(Suppl 1): S71–77.
2. Mann C, Honeyman K, Cheng A, Ly T, Lloyd F, et al. (2001) Antisense-induced exon skipping and synthesis of dystrophin in the mdx mouse. Proc Natl Acad Sci U S A 98: 42–47.
3. Alter J, Lou F, Rabinowitz A, Yin H, Rosenfeld J, et al. (2006) Systemic delivery of morpholino oligonucleotide restores dystrophin expression bodywide and improves dystrophic pathology. Nat Med 12: 175–177.
4. van Deutekom J, Janson A, Ginjaar I, Frankhuizen W, Aartsma-Rus A, et al. (2007) Local dystrophin restoration with antisense oligonucleotide PRO051. N Engl J Med 357: 2677–2686.
5. Kinali M, Arechavala-Gomeza V, Feng L, Cirak S, Hunt D, et al. (2009) Local restoration of dystrophin expression with the morpholino oligomer AVI-4658 in Duchenne muscular dystrophy: a single-blind, placebo-controlled, dose-escalation, proof-of-concept study. Lancet Neurol 8: 918–928.
6. Yokota T, Lu Q, Partridge T, Kobayashi M, Nakamura A, et al. (2009) Efficacy of systemic morpholino exon-skipping in Duchenne dystrophy dogs. Ann Neurol 65: 667–676.
7. Sharp N, Kornegay J, Van Camp S, Herbstreith M, Secore S, et al. (1992) An error in dystrophin mRNA processing in golden retriever muscular dystrophy, an animal homologue of Duchenne muscular dystrophy. Genomics 13: 115–121.
8. Béroud C, Tuffery-Giraud S, Matsuo M, Hamroun D, Humbertclaude V, et al. (2007) Multiexon skipping leading to an artificial DMD protein lacking amino acids from exons 45 through 55 could rescue up to 63% of patients with Duchenne muscular dystrophy. Hum Mutat 28: 196–202.
9. Wee K, Pramono Z, Wang J, MacDorman K, Lai P, et al. (2008) Dynamics of co-transcriptional pre-mRNA folding influences the induction of dystrophin exon skipping by antisense oligonucleotides. PLoS ONE 3: e1844.
10. Pramono Z, Takeshima Y, Alimsardjono H, Ishii A, Takeda S, et al. (1996) Induction of exon skipping of the dystrophin transcript in lymphoblastoid cells by transfecting an antisense oligodeoxynucleotide complementary to an exon recognition sequence. Biochem Biophys Res Commun 226: 445–449.
11. Chelly J, Gilgenkrantz H, Hugnot J, Hamard G, Lambert M, et al. (1991) Illegitimate transcription. Application to the analysis of truncated transcripts of the dystrophin gene in nonmuscle cultured cells from Duchenne and Becker patients. J Clin Invest 88: 1161–1166.
12. Aartsma-Rus A, Janson A, Kaman W, Bremmer-Bout M, den Dunnen J, et al. (2003) Therapeutic antisense-induced exon skipping in cultured muscle cells from six different DMD patients. Hum Mol Genet 12: 907–914.
13. Aartsma-Rus A, Janson A, Kaman W, Bremmer-Bout M, van Ommen G, et al. (2004) Antisense-induced multiexon skipping for Duchenne muscular dystrophy makes more sense. Am J Hum Genet 74: 83–92.
14. Gonçalves M, Swildens J, Holkers M, Narain A, van Nierop G, et al. (2008) Genetic complementation of human muscle cells via directed stem cell fusion. Mol Ther 16: 741–748.
15. Cooper S, Kizana E, Yates J, Lo H, Yang N, et al. (2007) Dystrophinopathy carrier determination and detection of protein deficiencies in muscular dystrophy using lentiviral MyoD-forced myogenesis. Neuromuscul Disord 17: 276–284.
16. Zheng J, Wang Y, Karandikar A, Wang Q, Gai H, et al. (2006) Skeletal myogenesis by human embryonic stem cells. Cell Res 16: 713–722.
17. McClorey G, Moulton H, Iversen P, Fletcher S, Wilton S (2006) Antisense oligonucleotide-induced exon skipping restores dystrophin expression in vitro in a canine model of DMD. Gene Ther 13: 1373–1381.
18. Reiss J, Rininsland F (1994) An explanation for the constitutive exon 9 cassette splicing of the DMD gene. Hum Mol Genet 3: 295–298.
19. Miller A, Buttimore C (1986) Redesign of retrovirus packaging cell lines to avoid recombination leading to helper virus production. Mol Cell Biol 6: 2895–2902.
20. Morgenstern J, Land H (1990) A series of mammalian expression vectors and characterisation of their expression of a reporter gene in stably and transiently transfected cells. Nucleic Acids Res 18: 1068.
21. Choi J, Costa M, Mermelstein C, Chagas C, Holtzer S, et al. (1990) MyoD converts primary dermal fibroblasts, chondroblasts, smooth muscle, and retinal pigmented epithelial cells into striated mononucleated myoblasts and multinucleated myotubes. Proc Natl Acad Sci U S A 87: 7988–7992.
22. Etzion S, Barbash I, Feinberg M, Zarin P, Miller L, et al. (2002) Cellular cardiomyoplasty of cardiac fibroblasts by adenoviral delivery of MyoD ex vivo: an unlimited source of cells for myocardial repair. Circulation 106: I125–130.
23. Noda T, Fujino T, Mie M, Kobatake E (2009) Transduction of MyoD protein into myoblasts induces myogenic differentiation without addition of protein transduction domain. Biochem Biophys Res Commun 382: 473–477.
24. Shimatsu Y, Yoshimura M, Yuasa K, Urasawa N, Tomohiro M, et al. (2005) Major clinical and histopathological characteristics of canine X-linked muscular dystrophy in Japan, CXMDJ. Acta Myol 24: 145–154.
25. Mitrpant C, Adams A, Meloni P, Muntoni F, Fletcher S, et al. (2009) Rational design of antisense oligomers to induce dystrophin exon skipping. Mol Ther 17: 1418–1426.
26. Aartsma-Rus A, Kaman W, Weij R, den Dunnen J, van Ommen G, et al. (2006) Exploring the frontiers of therapeutic exon skipping for Duchenne muscular dystrophy by double targeting within one or multiple exons. Mol Ther 14: 401–407.
27. Harding P, Fall A, Honeyman K, Fletcher S, Wilton S (2007) The influence of antisense oligonucleotide length on dystrophin exon skipping. Mol Ther 15: 157–166.
28. Aartsma-Rus A, van Ommen G (2007) Antisense-mediated exon skipping: a versatile tool with therapeutic and research applications. RNA 13: 1609–1624.
29. Wilton S, Fall A, Harding P, McClorey G, Coleman C, et al. (2007) Antisense oligonucleotide-induced exon skipping across the human dystrophin gene transcript. Mol Ther 15: 1288–1296.
30. McClorey G, Fall A, Moulton H, Iversen P, Rasko J, et al. (2006) Induced dystrophin exon skipping in human muscle explants. Neuromuscul Disord 16: 583–590.
31. Aartsma-Rus A, De Winter C, Janson A, Kaman W, Van Ommen G, et al. (2005) Functional analysis of 114 exon-internal AONs for targeted DMD exon skipping: indication for steric hindrance of SR protein binding sites. Oligonucleotides 15: 284–297.
32. Hallegger M, Llorian M, Smith C (2010) Alternative splicing: global insights. FEBS J 277: 856–866.
33. Sironi M, Cagliani R, Pozzoli U, Bardoni A, Comi G, et al. (2002) The dystrophin gene is alternatively spliced throughout its coding sequence. FEBS Lett 517: 163–166.
34. Pruitt K, Harrow J, Harte R, Wallin C, Diekhans M, et al. (2009) The consensus coding sequence (CCDS) project: Identifying a common protein-coding gene set for the human and mouse genomes. Genome Res 19: 1316–1323.
35. Desmet F, Hamroun D, Lalande M, Collod-Béroud G, Claustres M, et al. (2009) Human Splicing Finder: an online bioinformatics tool to predict splicing signals. Nucleic Acids Res 37: e67.

筋ジストロフィーの新しい治療戦略*

武田　伸一**

Key Words: Duchenne muscular dystrophy, dystrophin, exon skipping, dystrophic dog, mdx 52 mice

はじめに

筋ジストロフィーは「骨格筋の変性，壊死を主病変とし，臨床的には進行性の筋力低下をみる遺伝性の疾患である」と定義される．筋ジストロフィーの原因遺伝子の多くは筋細胞膜のタンパク質，中でもジストロフィン・糖タンパク質複合体（dystrophin-glycoprotein complex：DGC）の構成分子をコードしており，この複合体が骨格筋膜の安定性に重要である事を示唆する．デュシェンヌ型筋ジストロフィー（Duchenne muscular dystrophy：DMD）はDMD遺伝子の変異によりDGCの中心分子であるジストロフィンが欠損することで発症し，ジストロフィンの欠損が不完全な場合はベッカー型筋ジストロフィー（Becker type progressive muscular dystrophy：BMD）の表現型を呈する．DMDは，X染色体連鎖性遺伝形式をとり，筋ジストロフィーの中で最も頻度が高く，新生男児3,500人に1人の割合で発症する．DMD患者は2～5歳時に歩行異常で気付かれることが多く，進行性の筋力低下のため11～13歳前後に独立歩行が不可能になり，以後呼吸不全や心不全で死亡に至る．最近，呼吸管理の進歩により，約10年間寿命が延長しているが，有効と認められている治療は副腎皮質ステロイドと脊椎変形に対する手術，呼吸補助と心不全に対する薬物療法のみであり，未だ筋変性・壊死を阻止する決定的な治療法はない．そこで，先進的な治療である遺伝子治療，幹細胞移植治療を含めて，治療法の開発研究が世界各国で，極めて活発に進められている．

I．Anti-sense oligonucleotides（AOs）によるエクソン・スキップ

人工的に合成された短い核酸化合物であるAOsを用いて行われるエクソン・スキップ誘導療法では，pre mRNAからmRNAへのスプライシング過程で，遺伝子変異を持つ，あるいはその近傍のエクソンを人為的にスキップさせて，アウト・オブ・フレーム変異をイン・フレーム変異に変換することを企図する．誘導されるジストロフィンは，正常なジストロフィンのタンパク質構造を一部欠くことになるが，actin結合ドメインやcysteine-richドメイン，C端ドメインなどの重要な分子構造は保存される．

* New Therapeutic Strategies to Duchenne Muscular Dystrophy.

** 独立行政法人国立精神・神経医療研究センタートランスレーショナル・メディカルセンター・神経研究所遺伝子疾患治療研究部
Shin'ichi TAKEDA：Translational Medical Center, National Center of Neurology and Psychiatry. Department of Molecular Therapy, National Institute of Neuroscience, National Center of Neurology and Psychiatry

現在，筋ジストロフィーのモデル動物を用いたin vitroおよびin vivoでの研究や臨床治験に使用されている代表的なAOsには，2'-O-methyl phosphorothioate antisense oligoribonucleotide (2OMeAO)，phosphorodiamidate morpholino oligomer（PMOあるいはモルフォリノ）がある．特に，PMOは，ヌクレアーゼなど生体内の酵素による分解を受けずに，免疫応答を誘導しないPMO環構造を持つ水溶性の核酸類似人工化合物である[1,2]．しかも，塩基間の分子距離を維持するように設計されており，標的pre mRNAに対し非常に強い配列特異的結合を可能にしている一方，電荷を持たないため，細胞膜の通過性が低い点が課題として指摘されていた．

最近，国立精神・神経医療研究センターでコロニーを確立したDMDのモデル動物である筋ジストロフィー犬，CXMD$_J$[3]に対してPMOの筋肉内局所および全身投与が行われた[4]．筋ジストロフィー犬は，ジストロフィン遺伝子のイントロン6のスプライス・サイトに点変異を持ち，エクソン7をスキップしてエクソン8にストップ・コドンを生ずるため，ジストロフィンを発現していない．そこで，アミノ酸の読み枠を修正するためにエクソン6および8を標的とした合計3種類のAOsをカクテルにして投与を行った結果，心筋を除く全身骨格筋においてジストロフィンの発現が回復し，血清CK値も軽減し，病理組織学所見も改善した．また，PMO非投与の筋ジストロフィー犬と比較し，投与筋ジストロフィー犬では骨格筋のMRIで，筋の変性や壊死の改善が示唆され，運動機能をはじめとする臨床症状の改善も認められた．一方で，血液検査や諸臓器の病理組織学上，副作用の徴候は全く認められず，PMOおよび発現誘導されたジストロフィンに対する免疫反応は観察されなかった[4]．本研究により，複数のエクソンを同時にスキップすることが可能になったことから，エクソン・スキップの対象となるDMD患者の範囲が拡大し，遺伝子欠失によるDMDの約80%に達したことが特筆される．

エクソン6/8スキップ療法の限界の一つとしては，対象となる遺伝子変異を持つDMD患者の数が極めて限られていることが挙げられていた．ところが，DMD遺伝子エクソン7欠失を有するDMD患者が国内で見出された．患者本人及び家族の同意の下，国立精神・神経医療研究センター病院に入院して頂き，皮膚生検を実施することができた．生検材料から，線維芽細胞株を擁立し，MyoD遺伝子を導入して筋芽細胞に転換した上で，筋ジストロフィー犬で得られた配列を下に，PMOによるエクソン・スキップを試み，RT-PCR上でのエクソン6/8スキップと，免疫染色とWestern blotによるジストロフィンの発現を確認することができた．本研究により，モデル動物のみでなくDMD患者に於いてDMD遺伝子のエクソン6と8のスキップ療法を行う根拠が得られたものと考えている[5]．

II．エクソン・スキッピング治療の今後の見通しと問題点

DMD遺伝子のエクソン6/8スキップに関しては，前臨床試験を進め，DMD患者由来の細胞を用いたin vitro試験でも良好な結果が得られたとは言え，対象となる患者数に制限があることには疑いがない．そこでDMDで見出される変異が集中しているエクソン45から55の領域（所謂ホットスポット領域）に注目して検索したところ，エクソン51のスキップに成功すれば，遺伝子欠失によるDMD患者の約15%について，イン・フレーム化できることが明らかになった．しかし，それを実証するためには，疾患モデル動物を用いた検証が必要である．そこで，以前に我々からの要請に基づいて開発されたDMD遺伝子のエクソン52を欠いた筋ジストロフィーマウス（mdx52マウス）[6]を用いてエクソン51スキップが可能であって表現型を改善する効果があるかどうか検証した．最初にmdx52マウス前脛骨筋にPMOを筋注することによりエクソン51スキップが可能なアンチセンス配列の組み合わせを検証した．その上で，最適な組み合わせのPMOについて尾静脈経由の全身投与実験を行った．その結果，エクソン51スキップにより，心筋を除く全身の骨格筋でジストロフィンの発現が回復し血清CK値，筋張力，組織像をはじめとする表現型の改善が認められた．少なくともmdx52マウスにおいては，エクソン51スキップの有効性が検証されたと言える[7]．

現在，DMD患者に対する臨床治験として，オ

ランダやイギリスで，エクソン51を標的とした2OMeAOやPMOの全身投与が進められている．2OMeAOを用いた治験に関しては，6mg/kgの投与量で，皮下注による全身投与が行われ，比較的少数のDMD患児に対する24週までの投与では，6分間歩行試験において良好な臨床的な効果が得られている．一方で，蛋白尿等の懸念も指摘されている．PMOを用いた治験に関しては，比較的少数のDMD患児を対象に12週までの投与が行われた結果，投与量に応じてジストロフィンの発現が認められ，何ら毒性は観察されなかった．しかし，20mg/kgまでの投与の範囲では，臨床的な有効性が観察されなかったことが指摘されている．

ただし，これまでの研究結果からエクソン・スキッピング治療を臨床応用するために解決しなければならない問題点も明らかとなった．

1つのエクソンを標的としたシングル・エクソン・スキップは，治療対象となる患者数に限りがあり，しかもそれぞれの遺伝子変異に応じたAOsが必要となる（テーラーメイド治療）．そのため複数のAOsを混合して広範囲のエクソンをスキップさせるマルチ・エクソン・スキッピング療法が期待されている．この手法は，シングル・エクソン・スキップ療法よりも比較的多くのDMD患者をカバーすることができる．例えば，エクソン45-55の欠損患者のうち94%が軽症のBMDと報告されていることから，DMDのホットスポット変異として知られているエクソン45-55の範囲内に大小の欠失を持つDMD患者に対してエクソン45-55をまとめてスキップする共通した治療が可能となる．

一方，これまで検討されてきた2OMeAOやPMOでは，心筋での効率は低いことが指摘されている．近年，ペプチドの血清中や細胞内での安定性の増加，物質のエンドソームでのトラップの減少および核酸の細胞内への取り込みを増加させる目的で，PMOに細胞膜透過性ペプチド（CPPs）であるアルギニン，6-アミノヘキサン酸，および/またはβ-アラニンを付加したpeptide-linked PMO（PPMO）が開発された[8]．

III．結論

ジストロフィン欠損によるDMD患者に関しては呼吸不全，心不全対策の発展に伴い寿命が延長しているものの，疾患の本態に根ざした治療はいまだ確立されておらず，治療法の開発が急務である．近年，欧米ではDMD患者に対する臨床治験が開始され，その動きが日本にも及ぼうとしている．DMDに対する治療研究で開発された技術，特にPMOあるいは，筋ジストロフィーの他の病型のみならず，多くの遺伝性神経・筋疾患にも応用が期待される．

文　献

1）Nakamura A, Takeda S : Exon-skipping therapy for Duchenne muscular dystrophy. Neuropathology 29 : 494-501, 2009

2）Miyagoe-Suzuki Y, Takeda S : Gene therapy for muscle disease. Exp Cell Res 316 : 3087-3092, 2010

3）Urasawa N, Wada MR, Machida N et al : Selective vacuolar degeneration in dystrophin deficient canine Purkinje fibers despite preservation of dystrophin-associated proteins with overexpression of Dp71. Circulation 117 : 2437-2448, 2008

4）Yokota T, Lu QL, Partridge T et al : Efficacy of systemic morpholino exon-skipping in duchenne dystrophy dogs. Ann Neurol 65 : 667-676, 2009

5）Saito T, Nakamura A, Aoki Y et al : Antisense PMO Found in Dystrophic Dog Model Was Effective in Cells from Exon 7-Deleted DMD Patient. PLoS One 5 (8) : e12239, 2010

6）Araki E, Nakamura K, Nakao K et al : Targeted disruption of exon 52 in the mouse dystrophin gene induced muscle degeneration similar to that observed in Duchenne muscular dystrophy. Biochem Biophys Res Commun 238 : 492-497, 1997

7）Aoki Y, Nakamura A, Yokota T et al : In-frame dystrophin following exon 51-skipping improves muscle pathology and function in the exon 52-deficient mdx mouse. Mol Ther 18 : 1995-2005, 2010

8）Yokota T, Lu QL, Partridge TA et al : A renaissance for antisense oligonucleotide drugs in neurology : exon skipping breaks new ground. Arch Neurol 66 : 32-38, 2009

New Therapentic Strategies to Duchenne Muscular Dystrophy

Shin'ichi TAKEDA

Translational Medical Center, National Center of Neurology and Psychiatry
Department of Molecular Therapy, National Institute of Neuroscience,
National Center of Neurology and Psychiatry

Duchenne muscular dystrophy (DMD) is a lethal muscle disorder caused by the mutations of the DMD gene, which encodes a 427-kDa spectrin-like cytoskeletal protein, dystrophin. Exon skipping by antisense oligonucleotides is a novel method to restore the reading frame of the mutated DMD gene, and rescue dystrophin expression. We recently demonstrated that systemic delivery of Morpholino antisense oligonucleotides targeting exon 6 and 8 of the canine DMD gene, efficiently recovered functional dystrophin at the sarcolamma of dystrophic dogs, and improved performance of affected dogs without serious side effects (Yokota et al., Ann Neurol, 2009). We, then, experienced an exon 7-deleted DMD patient in Japan and got cultured fibroblasts from biopsy specimen. We converted these cells into myogenic cells by MyoD cDNA transfection and examined skipping efficiency of exon 6 and 8 of the DMD gene. We observed effective skipping of these exons and recovery of dystrophin expression on the cells (Saito et al., PLoS One, 2010) We also optimized antisense Morpholinos targeting exon 51 of the mouse DMD gene, to prepare clinical trials for the DMD patients with frequent mutations of the DMD gene. A combination of two Morpholinos showed an excellent restoration of sarcolemmal dystrophin in injected muscle or after systemic delivery, and amelioration of dystrophic pathology, and improvement of contractile force (Aoki et al., Mol Ther, 2010). Clinical trials of exon 51 skipping are under way in DMD patients at this moment.

Am J Physiol Endocrinol Metab 300: E543–E553, 2011.
First published January 4, 2011; doi:10.1152/ajpendo.00430.2010.

Follistatin-derived peptide expression in muscle decreases adipose tissue mass and prevents hepatic steatosis

Masashi Nakatani,[1] Masahiro Kokubo,[2] Yutaka Ohsawa,[3] Yoshihide Sunada,[3] and Kunihiro Tsuchida[1]

[1]Division for Therapies against Intractable Diseases, Institute for Comprehensive Medical Science (ICMS), and [2]Joint Research Laboratories, Fujita Health University, Toyoake; and [3]Division of Neurology, Department of Internal Medicine, Kawasaki Medical School, Kurashiki, Japan

Submitted 20 July 2010; accepted in final form 3 January 2011

Nakatani M, Kokubo M, Ohsawa Y, Sunada Y, Tsuchida K. Follistatin-derived peptide expression in muscle decreases adipose tissue mass and prevents hepatic steatosis. *Am J Physiol Endocrinol Metab* 300: E543–E553, 2011. First published January 4, 2011; doi:10.1152/ajpendo.00430.2010.—Myostatin, a member of the transforming growth factor (TGF)-β superfamily, plays a potent inhibitory role in regulating skeletal muscle mass. Inhibition of myostatin by gene disruption, transgenic (Tg) expression of myostatin propeptide, or injection of propeptide or myostatin antibodies causes a widespread increase in skeletal muscle mass. Several peptides, in addition to myostatin propeptide and myostatin antibodies, can bind directly to and neutralize the activity of myostatin. These include follistatin and follistatin-related gene. Overexpression of follistatin or follistatin-related gene in mice increased the muscle mass as in myostatin knockout mice. Follistatin binds to myostatin but also binds to and inhibits other members of the TGF-β superfamily, notably activins. Therefore, follistatin regulates both myostatin and activins in vivo. We previously reported the development and characterization of several follistatin-derived peptides, including FS I-I (Nakatani M, Takehara Y, Sugino H, Matsumoto M, Hashimoto O, Hasegawa Y, Murakami T, Uezumi A, Takeda S, Noji S, Sunada Y, Tsuchida K. *FASEB J* 22: 477–487, 2008). FS I-I retained myostatin-inhibitory activity without affecting the bioactivity of activins. Here, we found that inhibition of myostatin increases skeletal muscle mass and decreases fat accumulation in FS I-I Tg mice. FS I-I Tg mice also showed decreased fat accumulation even on a control diet. Interestingly, the adipocytes in FS I-I Tg mice were much smaller than those of wild-type mice. Furthermore, FS I-I Tg mice were resistant to high-fat diet-induced obesity and hepatic steatosis and had lower hepatic fatty acid levels and altered fatty acid composition compared with control mice. FS I-I Tg mice have improved glucose tolerance when placed on a high-fat diet. These data indicate that inhibiting myostatin with a follistatin-derived peptide provides a novel therapeutic option to decrease adipocyte size, prevent obesity and hepatic steatosis, and improve glucose tolerance.

myostatin; adipocyte; fatty liver; glucose tolerance

THE TRANSFORMING GROWTH FACTOR (TGF)-β superfamily is one of the largest families of secreted growth and differentiation factors and plays important roles in regulating tissue development and homeostasis (37). Myostatin, a member of the TGF-β superfamily, acts as a negative regulator of muscle growth (19, 22). Mutations in the myostatin gene in cattle, sheep, dogs, and humans cause an increase in skeletal muscle mass, indicating conservation of its function in mammals (5, 8, 23, 26, 32, 33). Myostatin is expressed predominantly in skeletal muscle and at significantly lower levels in adipose tissue (22). Inhibition of myostatin causes an increase in skeletal muscle mass and ameliorates several models of muscular dystrophies. Therefore, myostatin inhibitors are a promising therapeutic target to treat muscular atrophy and muscular dystrophy (19, 29, 37).

The loss of myostatin by gene disruption prevents an age-related increase in adipose tissue mass and partially attenuates the obese and diabetic phenotypes (14, 24). The serum leptin concentration and adipose tissue leptin mRNA expression were lower in myostatin null mice than in wild-type mice (24). Inhibition of myostatin by transgenic (Tg) expression of myostatin propeptide was also reported to prevent diet-induced obesity (41, 42). Even when fed a high-fat diet (HFD), these mice exhibited normal insulin sensitivity, unlike wild-type mice (42). Furthermore, ΔACVR2B, a soluble extracellular form of the activin type IIB receptor, effectively decreased the adipose tissue mass (1). These results suggest that inhibition of myostatin signaling could be useful to prevent and/or treat obesity and diabetes.

There are several strategies to block the functions of myostatin, including myostatin propeptide, follistatin, follistatin-related gene (FLRG), follistatin domain-containing growth and differentiation factor-associated serum protein-1 (GASP-1), the potent myostatin inhibitor ΔACVR2B, neutralizing antibodies, and small chemical compounds that block receptor serine kinases (2, 15, 37, 38).

Follistatin was shown to bind to myostatin and inhibit its activity. However, follistatin inhibits other members of the TGF-β superfamily, including GDF11 and activin (11, 37, 38). Although GDF11 and myostatin show a high degree of sequence similarity at the amino acid level, GDF11 is unlikely to regulate skeletal muscle mass, because GDF11 controls skeleton and kidney development rather than regulating muscle mass (21). Like myostatin, activin regulates skeletal muscle mass (12). However, unlike myostatin, activin has many pleiotropic roles including ovarian and neuronal functions (30, 36). In our previous study, we reported the development and characterization of a myostatin inhibitor derived from follistatin, designated FS I-I. FS I-I is unable to neutralize activin but still binds to and inhibits myostatin (27). Tg expression of FS I-I using a skeletal muscle-specific promoter caused a widespread increase in skeletal muscle mass and ameliorated muscular dystrophy. In addition, muscle strength was recovered when the FS I-I Tg mice were crossed with *mdx* mice (27). In this study, we explored whether FS I-I Tg mice are resistant to diet-induced obesity and hepatic steatosis. We found that FS I-I Tg mice exhibited reduced fat accumulation even when fed a normal diet (NFD). Adipocytes were also much smaller than those of wild-type littermates. Furthermore, the FS I-I Tg mice

Address for reprint requests and other correspondence: K. Tsuchida, Division for Therapies against Intractable Diseases, Institute for Comprehensive Medical Science (ICMS), Fujita Health Univ., Toyoake, Aichi 470-1192, Japan (e-mail: tsuchida@fujita-hu.ac.jp).

were resistant to HFD-induced obesity and hepatic steatosis. The liver of HFD-fed FS I-I Tg mice showed significantly different fatty acid composition compared with that seen in the control mice. Our studies suggest that follistatin-derived myostatin inhibitors offer a therapeutic option for obesity, diabetes, and hepatic steatosis.

MATERIALS AND METHODS

Animals. The establishment of skeletal muscle-specific FS I-I Tg mice is described in our previous paper (27). In brief, *Eco*RI-*Sma*I fragment covering the whole coding sequence of FS I-I was subcloned into the MDAF2 vector containing the myosin light-chain promoter SV40 processing sites and MLC1/3 enhancer. *Cla*I fragment with 3.9 kb was microinjected to produce FS I-I transgenic mice (27). The transgene was expressed in skeletal muscles but not in cardiac muscle or adipose tissues. FS I-I Tg male mice and wild-type littermates were obtained from the offspring of FS I-I Tg mice mated with C57BL/6 mice. The genotypes were determined by PCR as previously described (27). The FS I-I Tg and littermate male mice were weaned at 4 wk of age and given free access to either a normal-fat (NFD; 5% kcal fat; CE-2; CLEA, Shizuoka, Japan) or a high-fat diet (HFD; 32% kcal fat, High Fat Diet 32, CLEA) from 4 to 13 wk. Food intake did not differ between the two genotypes on the HFD. Body weight was recorded every week. All mice were housed in cages with a constant temperature (22°C) and a 12:12-h light-dark cycle. All experiments were performed at the Laboratory Animal Center with approval from the Animal Research Committee at Fujita Health University.

Analysis of adipose tissue, skeletal muscle, and liver. Adipose tissues (retroperitoneal, epididymal, and inguinal fat pads), skeletal muscles [tibialis anterior (TA), extensor digitorum longus (EDL), quadriceps femoris (Qf), and soleus], and liver samples were obtained from mice at 13 or 20 wk of age. Adipose tissue and muscles were also obtained from NFD- and HFD-fed mice at *week 13*. The wet tissue weights were measured.

Histological analyses of adipose tissues and liver. The adipose tissues and livers either from FS I-I Tg mice or littermates were fixed in 4% paraformaldehyde (PFA), dehydrated in ethanol, embedded in paraffin, and sectioned at a thickness of 6 μm. The sections were then deparaffinized, rehydrated, and stained with hematoxylin and eosin (H&E). The area of adipocytes was determined in images stained with H&E. The area of 200 adipocytes per mouse was determined in five wild-type and five FSI-I Tg mice (1,000 adipocytes for each genotype), and the average cell area was determined. Morphometric analyses to measure adipocyte area and size were performed using WinROOF software (Mitani, Fukui, Japan).

Electron microscope analysis. Adipose tissue samples were fixed for 4 h with 2% PFA and 2.5% glutaraldehyde in phosphate-buffered saline (PBS) at room temperature. The specimens were then postfixed at room temperature for 1 h with 2% osmium tetroxide in Millonig's buffer containing 0.54% glucose and dehydrated through an ethanol gradient. For scanning electron microscopy, the dehydrated specimens were then immersed in *t*-butyl alcohol, dried using a freeze-drying device, coated with gold using an ion sputtering device (JEE-420T, JEOL), and examined under a scanning electron microscope (H7650; Hitachi, Tokyo, Japan). For transmission electron microscopy, specimens were immersed in QY-1 (Nisshin EM, Tokyo, Japan), embedded in epoxy resin (Epon812; Polyscience, Wako Pure Chemical Industries, Osaka, Japan), and cut into ultrathin sections. The sections were stained with uranyl acetate and lead citrate, followed by transmission electron microscopy at an accelerating voltage of 80 kV (JEM-1010TEM, JEOL). One hundred fifty mitochondria of epididymal adpipocytes each from three wild-type and FS I-I Tg mice were analyzed using WinROOF software.

Quantitative real-time PCR. The relative expressions of uncoupling protein-3 (UCP3), acetyl-CoA carboxylase-1 (ACC1), stearoyl-CoA desaturase-1 (SCD1), glucokinase (Gck), and phosphofructokinase (PFK) were determined by quantitative (q)PCR using a TAKARA Thermal Cycler Dice Real-Time System (Takara Bio, Shiga, Japan). Briefly, mRNA was isolated from liver and adipose tissues from FS I-I Tg mice and wild-type littermates by use of TRIzol (Invitrogen, Tokyo, Japan) with standard techniques. The isolated RNA was cleaned by DNaseI and purified using RNeasy Tissue kits (Qiagen, Tokyo, Japan). Reverse transcription was carried out with 500 ng of RNA using QuantiTect reverse transcription kits (Qiagen) according to the manufacturer's instructions.

We used Primer 3 software to design the primers for UCP3 (forward: 5′-CCGGTGGATGTGGTAAAGAC-3, reverse: 5′-AAGCTCCCAGACGCAGAAAG-3); ACC1 (forward: 5′-CCCATCCAAACAGAGGGAAC-3, reverse: 5-CTGACAAGGTGGCGTGAAG-3); SCD1 (forward: 5′-CAAGCTGGAGTACGTCTGGA-3′, reverse: 5′-CAGAGCGCTGGTCATGTAGT-3′); Gck (forward: 5′-TGGGCTTCACCTTCTCCTTC-3′, reverse: 5′-CGATGTTGTTCCCTTCTGCT-3′); and PFK (forward: 5′-GAAGCCAATCACCTCAGAAGAC-3′, reverse: 5′-TTCCACACCCATCCTGCT-3′). Each well of the 96-well reaction plate contained a total volume of 25 μl. cDNA (0.5 μl) solution was combined with each of forward and reverse primers (10 μM), distilled water, and SYBR Premix Ex Taq (Takara Bio). All reactions were performed in triplicate. The relative amounts of RNAs were calculated using the comparative C_T method. We used hepatic glyceraldehyde-3-phosphate dehydrogenase (GAPDH) and adipose tissue 36B4 as controls. Significant differences between the wild-type and FS I-I Tg mice were analyzed by Student's *t*-test.

Western blotting. Adipose tissues (epididymal and inguinal fat pads), skeletal muscle (Qf), and liver were dissected from wild-type and FSI-I Tg mice. Samples were homogenized in a buffer containing 50 mM Tris·HCl, pH 7.5, 150 mM NaCl, 5 mM NaF, 1% Nonidet P-40, 5 mM β-glycerophosphate, 1 mM phenylmethylsulfonyl fluoride, 4 μg/ml leupeptin, and 1 μg/ml aprotinin and centrifuged at 15,000 rpm for 10 min at 4°C, and the lipid-free lysates were collected. Aliquots of the lysates containing 30 μg of protein or serum containing 60 μg of protein were separated by sodium dodecyl sulfate-polyacrylamide gel electrophoresis and transferred onto polyvinylidene difluoride membranes. The membrane was blocked in 5% skim milk for 1 h at room temperature. The membranes were then probed with anti-cytochrome *c*, phosphorylated Smad 3, or Smad 3 (Cell Signaling Technology, Beverly, MA) at 4°C overnight (1:1,000 dilution), followed by incubation with horseradish peroxidase-conjugated secondary antibodies and chemiluminescence reactions by ECL plus (GE Healthcare, Tokyo, Japan). As a loading control, antibodies to tubulin or actin (Cell Signaling Technology, Beverly, MA) were used. Detection of FS I-I or follistatin by Western blotting was performed using rabbit polyclonal antibodies (ABPIII) raised against follistatin domain I of follistatin (31). Images of the developed immunoblots were captured using a cooled CCD camera system (Light-Capture; ATTO, Tokyo, Japan).

Measurement of serum parameters and triglycerides. Wild-type and FS I-I Tg mice (n = 4–6 per group) fed the NFD or HFD from *weeks 4* to *13* of age were fasted overnight at *week 13* for 16 h before blood sampling. The triglyceride, nonesterified fatty acid (NEFA), cholesterol, fasting glucose, insulin, leptin, and adiponectin concentrations were measured in serum samples prepared from whole blood collected from the retroorbital venous plexus of anesthetized mice. Plasma, total cholesterol, and NEFA were measured using enzymatic assays (triglyceride E, cholesterol E, and NEFA tests, respectively; Wako Pure Chemical Industries, Osaka, Japan). Plasma leptin, adiponectin, and insulin levels were measured using enzyme-linked immunoassays from Morinaga (Kanagawa, Japan), R&D systems (Gunma, Japan), and Otsuka (Tokyo, Japan), respectively. Triglycerides from liver and skeletal muscle were extracted with chloroform-methanol (2:1, vol/vol), centrifuged twice to remove debris, dried, and resuspended in 2-propanol containing 10% Triton X-100 (17). Triglyceride contents were enzymatically measured using a triglyceride E test. Mouse preadipocyte 3T3-L1 cells and human hepatocyte Hep

G2 cells were grown in Dulbecco's modified Eagle's medium (DMEM) supplemented with 10% fetal calf serum. Cells (1×10^5)/12-well plates of differentiating 3T3-L1 cells were stimulated with either 80 ng/ml FS I-I or 40 ng/ml myostatin (R&D systems) for 3 days. Hep G2 cells treated with 3 mg/ml glucose, 10 μg/ml insulin, and either 80 ng/ml FS I-I or 40 ng/ml myostatin for 3 days. Cellular triglycerides were extracted and measured as described above. All assays were performed according to the manufacturer's protocol.

Glucose tolerance test. Glucose tolerance tests were performed in six to eight mice per group at 13 wk of age after being fed the NFD or HFD for 9 wk. The mice were fasted overnight and then received an intraperitoneal injection of 10% dextrose (1 g/kg body wt). Blood was collected from the tail at 0, 15, 30, 60, and 120 min after dextrose injection, and blood glucose was measured using an Accu-Check glucose monitor (Roche Diagnostic, Indianapolis, IN).

Insulin tolerance test. Insulin tolerance tests were performed in five mice per group at 13 wk of age after being fed the HFD for 9 wk. The mice were starved for 16 h and received an intraperitoneal injection of human insulin (0.75 U/kg body wt; Sigma-Aldrich Japan). Blood glucose was measured at 0, 30, 60, and 90 min after injection using an Accu-Check glucose monitor (24).

Measurement of hepatic fatty acid content. Approximately 100 mg of liver tissue was obtained from wild-type and FS I-I Tg mice fed the NFD or HFD for 9 wk ($n = 6$ per group). Lipids were extracted using the Bligh-Dyer chloroform-methanol method (4). The extracted lipids were dissolved in 1 ml of chloroform and subjected to methanolysis-gas chromatographic analysis (3). Methyl stearate was used to generate a standard curve for quantitation. The determinations were repeated at least twice, and essentially the same results were obtained.

Metabolic rate analysis. Oxygen consumption was measured with an indirect calorimetric metabolism measuring system (model MK-5000RQ, Muromachikikai) (17). Each mouse was kept in a sealed chamber with an air flow of 0.6 l/min for 2 h during the light cycle. Air was sampled every 3 min, and the consumed oxygen concentration ($\dot{V}O_2$) was calculated (24). Five mice each for wild-type and FS I-I Tg mice fed NMD were analyzed.

Statistical analysis. Results are presented as means ± SD. Statistical significance was assessed by Student's *t*-tests. Differences between groups were considered statistically significant at $P < 0.05$. *P* values are presented in figure and table legends.

RESULTS

Decreased fat accumulation in FS I-I tg mice. We previously reported (27) that FS I-I Tg mice show a marked increase in skeletal muscle mass compared with wild-type mice when fed a NFD. Intriguingly, even with a NFD, FS I-I Tg mice showed age-dependent decreased fat accumulation. Although there was no difference in individual fat pad weights between wild-type and FS I-I Tg mice at 13 wk of age (data not shown), there was a significant difference at 20 wk of age. For example, at 20 wk of age, the weight of the epididymal fat pad was 60% lower in FS I-I Tg mice than in wild-type mice (Fig. 1*A*). Furthermore, the weights of the inguinal and retroperitoneal fat pads of FS I-I Tg mice were 33 and 67% lower, respectively, in FS I-I Tg mice than in wild-type mice. Therefore, we quantified the adipocyte size histologically using H&E staining (Fig. 1*B*)

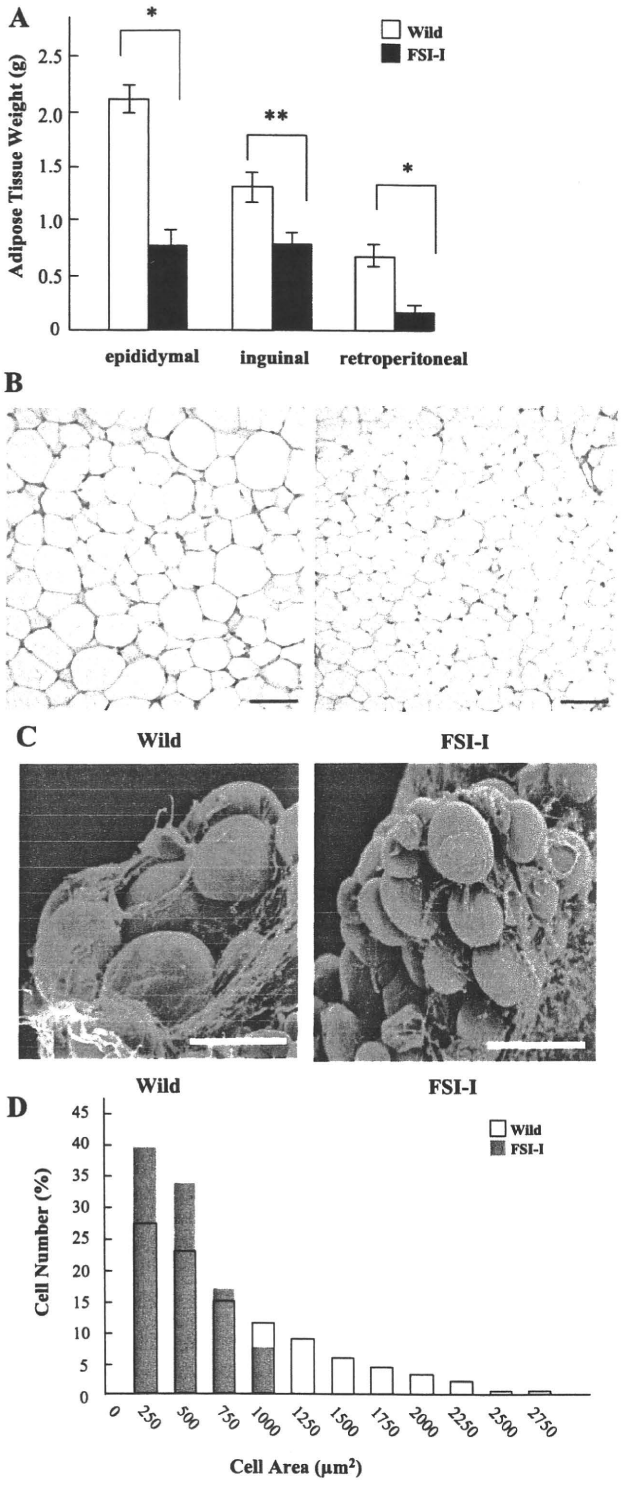

Fig. 1. *A*: adipose tissue weights (g) of 20-wk-old male wild-type and transgenic (Tg) mice with a myostatin inhibitor derived from follistatin [follistatin (FS)-derived peptide (FS I-I)] fed a control diet. Epididymal, inguinal, and retroperitoneal fat pads from 5 mice each from wild-type and FSI-I Tg mice were dissected and weighed. $*P < 0.005$ and $**P < 0.03$, Student's *t*-test. *B*: histological analysis of adipose tissues. Epididymal fat pads from 20-wk-old wild-type and FS I-I Tg mice were sectioned and stained with H&E. Scale bar, 100 μm. *C*: scanning electron microscopy of epididymal fat pads. 20-wk-old wild-type (*left*) and FS I-I Tg mice (*right*) were analyzed. Scale bar, 120 μm. *D*: distribution of epididymal adipocyte area in 20-wk-old wild-type and FS I-I Tg mice; 200 adipocytes were counted per mouse (5 mice per group). The percentage of adipocytes with indicated areas per total adipocytes was calculated and plotted. The mean adipocyte area was smaller in FS I-I Tg mice (717.4 ± 579.1 μm^2) than in wild-type mice (436.8 ± 309.1 μm^2).